

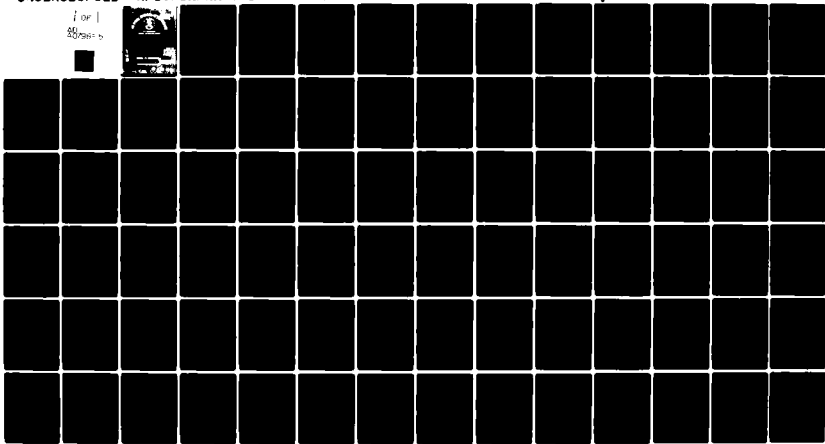
AD-A079 855

AIR FORCE INST OF TECH WRIGHT-PATTERSON AFB OH SCHOO--ETC F/G 22/1
USE OF AN AERODYNAMIC TURN TO MAXIMIZE THE ORBIT INCLINATION CH--ETC(U)
DEC 79 @ S GEARY
AFIT/GA/AA/79D-4

UNCLASSIFIED

NL

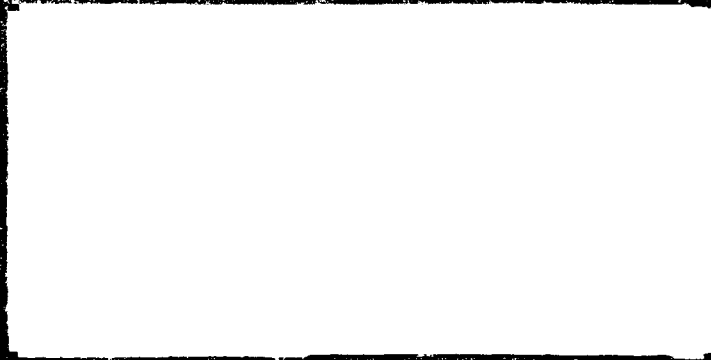
For
30 days



END
DATE
FILMED
2-80

DDC

ADA 079855



14

AFIT/GA/AA/79D-4

ADA 079855

9 *Mach's Thrust*

6

USE OF AN AERODYNAMIC TURN TO
MAXIMIZE THE ORBIT INCLINATION
CHANGE FOR THE SPACE SHUTTLE ORBITER

THESIS

AFIT/GA/AA/79D-4

10
Glenn S. Geary
Capt USAF

D D C
RECEIVED
NOV 1979

11 *Nov 79*

ADC FILE COPY

Approved for public release; distribution unlimited

183

019,925

47

AFIT/GA/AA/79D-4

USE OF AN AERODYNAMIC TURN TO
MAXIMIZE THE ORBIT INCLINATION
CHANGE FOR THE SPACE SHUTTLE ORBITER

THESIS

Presented to the Faculty of the School of Engineering
of the Air Force Institute of Technology
Air University
in Partial Fulfillment of the
Requirements for the Degree of
Master of Science

by

Glenn S. Geary, B.S.
Capt USAF

Graduate Astronautical Engineering

December 1979

Approved for public release; distribution unlimited

Accession For	
NTIS GRA&I	<input checked="" type="checkbox"/>
DDC TAB	<input type="checkbox"/>
Unannounced	<input type="checkbox"/>
Justification	
By _____	
Distribution/	
Availability Codes	
Dist.	Avail and/or special
A	

Preface

I would like to express my gratitude to Captains James Rader and William Wiesel. Their ready advice and endless patience was essential to the successful solution of this problem. Special thanks go to 2LT Gail Nusz for the hours she spent editing and typing the final report.

Glenn S. Geary

Contents

	<u>Page</u>
Preface.....	ii
List of Figures.....	v
List of Tables.....	vi
List of Notation.....	vii
Abstract.....	viii
I. Introduction.....	1
Background.....	1
Problem Statement and Scope.....	3
II. System Dynamics and Model Atmosphere.....	5
Background.....	5
Coordinate Reference Frame.....	5
Equations of Motion.....	8
Assumptions.....	9
Lift and Drag Computations.....	10
Model Atmosphere.....	11
Summary.....	17
III. Optimization Technique.....	18
Background.....	18
Optimal Control.....	18
Suboptimal Control.....	20
Second-Order Parameter Optimization.....	22
IV. Optimization Starting Values.....	25
Orbit Selection.....	26
Initial Position and Velocity Selection.....	28
Control Coefficient Selection.....	29
V. Results and Conclusions.....	35
Optimization Analysis.....	35
Apogee Analysis.....	36
Higher Order Control Analysis.....	44
Bibliography.....	51

	<u>Page</u>
APPENDIX A: Lockheed Bridging Formula.....	52
APPENDIX B: Optimization Program Listing.....	54
VITA	71

List of Figures

<u>Figure</u>	<u>Page</u>
1. Earth-Orbiter System Coordinate Frames.....	6
2. Initial and Final Angular Momentum Vectors.....	19
3. Control History - One Control Parameter.....	47
4. Control History - Three Control Parameters.....	48
5. Control History - Five Control Parameters.....	49
6. Control History - Seven Control Parameters.....	50
7. Optimization Program Flowchart.....	56

List of Tables

<u>Table</u>	<u>Page</u>
I. Orbiter Lift Coefficients.....	13
II. Orbiter Lift Coefficients - Concluded.....	14
III. Orbiter Drag Coefficients.....	15
IV. Orbiter Drag Coefficients - Concluded.....	16
V. Inclination Changes Obtained From Previous Research.....	25
VI. Reference Orbit Elements.....	27
VII. Initial Position and Velocity in Inertial Frame	30
VIII. End Condition Miss Errors 80/300 Orbit.....	32
IX. End Condition Miss Errors 80/500 Orbit.....	33
X. End Condition Miss Errors 80/650 Orbit.....	34
XI. Inclination Change Using Rocket Motor.....	38
XII. Maximum Orbit Plane Change ($\Delta v = 60$ mps).....	38
XIII. Velocity of Orbiter at Perigee.....	39
XIV. Time Inside Atmosphere.....	39
XV. VBAR History in Atmosphere ($\Delta v = 60$ mps).....	40
XVI. L/D Ratios Inside Atmosphere ($\Delta v = 60$ mps).....	40
XVII. Inclination Change For Various Velocity Losses (80/500 Orbit).....	41
XVIII. L/D Ratios versus Angle of Attack (Perigee VBAR)	43

List of Notation

- α = semi-major axis
 a = angle of attack
 C_L = coefficient of lift
 C_D = coefficient of drag
 e = eccentricity
 ϵ = specific mechanical energy
 H = angular momentum
 i = inclination
 Δi = change in inclination
 M = vector of prescribed final conditions
 p = semi-latus rectum
 ρ = local atmospheric density
 ϕ = angle of bank
 r_p = distance from earth center to perigee
 S = reference area
 T_1 = transformation matrix
 TP = orbital period
 μ = earth gravitational parameter
 v = scalar velocity in inertial frame
 V_{rel} = freestream velocity relative to orbiter
 Δv = change in velocity
 $VBAR$ = viscous parameter
 ν = true anomaly and Lagrange multiplier constants
 $\vec{\omega}$ = angular velocity of earth

Abstract

Previous studies have shown that the Space Shuttle Orbiter can achieve larger orbit inclination changes using an aerodynamic turn than can be obtained using a rocket motor burn. This analysis determines the angle of attack and bank angle histories which maximize the change in inclination angle while satisfying final altitude and velocity loss constraints. The angle of attack and bank angle are modelled as polynomial functions of time with unknown coefficients. The optimum values of the coefficients are determined by a gradient optimization technique. Additionally, the sensitivity of the change in inclination angle to changes in the orbit apogee altitude is examined. It is shown that the Space Shuttle Orbiter can obtain higher inclination angle changes from orbits with higher apogee altitudes.

USE OF AN AERODYNAMIC TURN TO
MAXIMIZE THE ORBIT INCLINATION
CHANGE FOR THE SPACE SHUTTLE ORBITER

I. Introduction

Background

When the Space Shuttle Orbiter becomes operational, new spacecraft capabilities will become available to space mission planners. Not only is the orbiter reusable, but for the first time mission planners will also have a spacecraft with significant aerodynamic capabilities. In certain regimes, the orbiter has a lift to drag ratio near two. When operating in this regime, the shuttle has the option of orienting the lift vector so that a change in orbit inclination is now possible via an aerodynamic turn rather than the conventional rocket motor burn method. What this offers the mission planner is a twofold capability. One, the orbiter can use the aerodynamic turn to increase the number of maneuvers possible during the course of a mission which would allow the servicing of more satellites. Secondly, the shuttle may trade fuel for increased payload at launch and still be able to accomplish a required minimum number of orbital maneuvers using the aerodynamic turn.

It is desirable to use the aerodynamic turn to achieve an inclination change if the maneuver is more efficient than the conventional rocket motor technique. The aerodynamic turn is more efficient than the rocket burn

if one of the following two conditions are met: (1) either the aerodynamic turn requires less velocity loss due to air drag (Δv) to achieve the same inclination change or (2) more of an inclination change is available for the same velocity loss when comparing the aerodynamic turn to the rocket burn.

If the aerodynamic turn is more efficient than the rocket burn, the orbiter will have several new options. First, the shuttle can use the aerodynamic turn to achieve an inclination change and then use the rocket motor to regain the velocity lost to aerodynamic drag. The end result would be a larger orbit inclination change than would be possible using only the rocket motor. Using this method, the shuttle orbit would have the same shape, but a new inclination. Secondly, the shuttle could use both the aerodynamic turn and the rocket motor to achieve a larger inclination change than is possible by either method alone. The resulting orbit would have not only a new inclination, but a different shape. Obviously, many variations of these two extremes are also available.

Previous research (Ref 5) shows that for perigee altitudes of 85 km and lower, the aerodynamic turn maneuver does achieve the same inclination change for less Δv cost than the rocket motor burn. This earlier study on the aerodynamic turn attempted to optimize the angle of attack and bank angle control history which minimized the work done by air drag (Δv) while satisfying end conditions

that specified final altitude and orbit inclination change. Because of this approach to the problem, the optimization technique did not function properly and a non-optimum approach to the efficiency of the aerodynamic turn was finally taken. The aerodynamic turn maneuver was found to be more efficient than the rocket motor burn and the maximum orbit inclination change obtained by the aerodynamic turn using a constant angle of attack and bank angle throughout the maneuver was $.78^{\circ}$. This earlier study recommended that research be continued on the subject with a restructured optimization problem and that the aerodynamic turn maneuver be limited to 95 km and lower perigee altitudes.

Problem Statement and Scope

This current investigation seeks, first, to find another approach to the optimization problem so that the difficulties encountered in the previous research (Ref 5: 49-50) are eliminated. If the problem can be successfully restated so that optimization is possible, the maximum orbit inclination change obtainable using the aerodynamic turn maneuver is desired.

The aerodynamic turn optimization problem is therefore restated as follows: Find the angle of attack and bank angle histories which maximize inclination change while satisfying end conditions that require returning the shuttle to a given final altitude with a specified acceptable velocity loss due to air drag.

Because the shuttle must obey the appropriate equations of motion during the aerodynamic turn maneuver, the maximization of inclination change is an optimal control problem. While there are several ways to solve an optimal control problem, the one chosen here is the Second-Order Control Parameter technique (Ref 7). In this method the orbiter controls are represented suboptimally as polynomial functions of time. The coefficients of the polynomials are chosen to optimize the performance index (maximum inclination change) and satisfy the end conditions (final altitude and velocity). Higher order control polynomials are investigated to determine their effect on inclination change and what order controls are necessary to accurately approximate the optimal controls. Additionally, a sensitivity analysis is conducted on various apogee altitudes to determine their effect on inclination change.

The remainder of this paper is arranged in the following manner: Chapter II discusses the orbiter equations of motion and the model atmosphere used in this study. Explanations of the methods used to generate coefficients of lift and drag are also given. Chapter III covers the optimization routine used, why it was selected and how it is implemented. Chapter IV reports on how the initial values of control coefficients and end conditions used in the optimization routine are selected. Chapter V lists the results and conclusions generated by this study.

II. System Dynamics and Model Atmosphere

Background

The Space Shuttle Orbiter is a dynamic system and must, therefore, obey Newton's laws of motion. Specifically, Newton's second law relates the aerodynamic and gravitational forces acting on the orbiter to the orbiter acceleration, $\Sigma F=ma$. This relationship can be expressed as a set of differential equations which describe the motion of the shuttle as it passes through the atmosphere. Before these equations of motion can be derived, a coordinate reference frame must be specified.

Coordinate Reference Frame

For this study, two coordinate reference frames are specified. The first, an X, Y, Z frame is earth centered, non-rotating, and inertial (Fig 1). The X, Y axes are in the earth equatorial plane and Z is chosen to complete a right-hand coordinate frame.

The second frame is the V_{rel}, M, L which is fixed at the center of mass of the orbiter (Fig 1). The V_{rel} axis points into the relative wind and the angle between the V_{rel} axis and the shuttle's longitudinal axis is the orbiter angle of attack α . The M axis establishes a local horizontal for the shuttle and L is chosen to complete the right-hand coordinate frame. The angle between the shuttle lift vector and the L axis establishes the angle of bank ϕ .

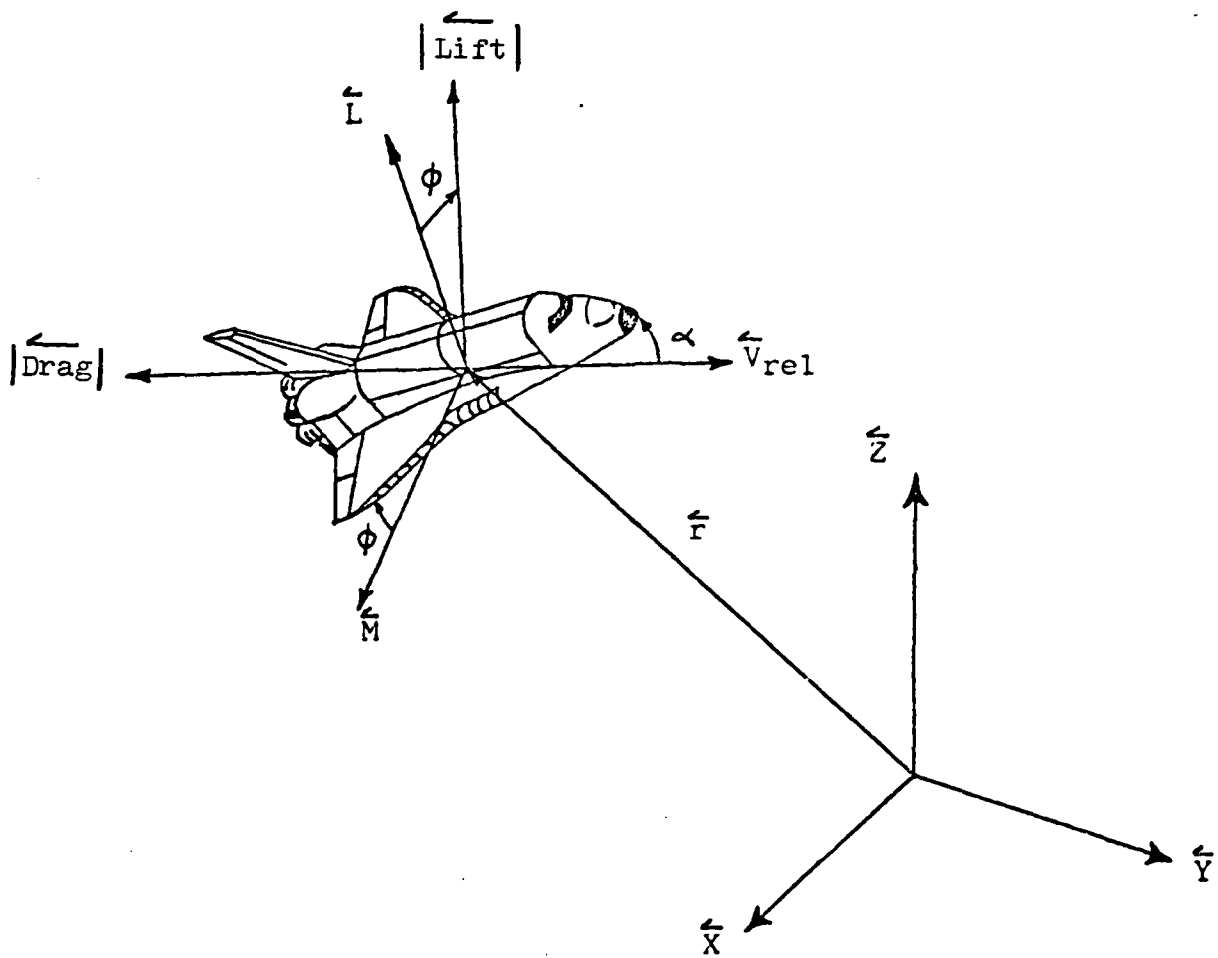


Figure 1, Earth-orbiter system coordinate frames

The Orbiter's aerodynamic forces are readily expressed in terms of the body fixed frame. These forces are

$$\begin{aligned}\vec{\text{LIFT}} &= |\vec{\text{LIFT}}| (\cos\phi\hat{\text{L}} - \sin\phi\hat{\text{M}}) \\ \vec{\text{DRAG}} &= |\vec{\text{DRAG}}| \hat{\text{V}}_{\text{rel}}\end{aligned}$$

where $|\vec{\text{LIFT}}|$ and $|\vec{\text{DRAG}}|$ represent the scalar magnitude of the lift and drag vector, respectively. $\hat{\text{V}}_{\text{rel}}$, $\hat{\text{M}}$, and $\hat{\text{L}}$ are unit vectors of the $\vec{\text{V}}_{\text{rel}}$, M, L frame. The position and velocity of the orbiter expressed in terms of X, Y, Z frame unit vectors is

$$\begin{aligned}\vec{r} &= X\hat{\text{I}} + Y\hat{\text{J}} + Z\hat{\text{K}} \\ \vec{v} &= \dot{X}\hat{\text{I}} + \dot{Y}\hat{\text{J}} + \dot{Z}\hat{\text{K}}\end{aligned}$$

where X, Y, Z, \dot{X} , \dot{Y} , and \dot{Z} are the system state variables.

The $\vec{\text{V}}_{\text{rel}}$, M, L vectors can be expressed as

$$\begin{aligned}\vec{\text{V}}_{\text{rel}} &= \vec{v} + \omega \times \vec{r} \\ \vec{\text{M}} &= \vec{\text{V}}_{\text{rel}} \times \vec{r} \\ \vec{\text{L}} &= \vec{\text{M}} \times \vec{\text{V}}_{\text{rel}}\end{aligned}$$

where ω = earth angular velocity. Substitution of the expressions for \vec{r} and \vec{v} into these equations allows $\vec{\text{V}}_{\text{rel}}$, M, and L to be expressed in terms of the state variables and the inertial frame unit vectors. This information allows the generation of a transformation matrix T, which will convert forces expressed in terms of the body frame to forces expressed in the inertial reference frame (Ref 5:16).

Equations of Motion

In addition to lift and drag, there is also a gravity force acting on the orbiter. The forces acting on the shuttle expressed in the inertial frame are:

$$\vec{\Sigma F} = \vec{\text{Gravity}}_{XYZ} + \vec{\text{Lift}}_{XYZ} + \vec{\text{Drag}}_{XYZ}$$

However, drag and lift forces are expressed in the body frame and will have to be converted to the inertial frame using the transformation matrix T. Therefore, the summation of forces is rewritten as:

$$\vec{\Sigma F} = \vec{\text{Gravity}}_{XYZ} + T(\vec{\text{Lift}}_{V_{rel}^{ML}}) + T(\vec{\text{Drag}}_{V_{rel}^{ML}})$$

The aerodynamic forces listed above can be written as three second-order differential equations (Ref 5:17). These equations can be further reduced to six first-order equations which become the shuttle equations of motion. These equations of motion are listed below.

Letting

$$\begin{aligned} w_1 &= X \\ w_2 &= Y \\ w_3 &= Z \\ w_4 &= \dot{X} \\ w_5 &= \dot{Y} \\ w_6 &= \dot{Z} \end{aligned}$$

the equations of motion are

$$\begin{aligned} \dot{w}_1 &= w_4 \\ \dot{w}_2 &= w_5 \\ \dot{w}_3 &= w_6 \end{aligned}$$

$$\begin{aligned}\dot{w}_4 &= -(GM/r^3)X + (\overset{\rightarrow}{\text{LIFT}}/M)T_1 - (\overset{\rightarrow}{\text{DRAG}}/M)T_2 \\ \dot{w}_5 &= -(GM/r^3)Y + (\overset{\rightarrow}{\text{LIFT}}/M)T_3 - (\overset{\rightarrow}{\text{DRAG}}/M)T_4 \\ \dot{w}_6 &= -(GM/r^3)Z + (\overset{\rightarrow}{\text{LIFT}}/M)T_5 - (\overset{\rightarrow}{\text{DRAG}}/M)T_6\end{aligned}$$

where T_i $i = 1$ to 6 is the appropriate element of the transformation matrix (Ref 5:18).

Assumptions

The equations of motion listed above are based on the following assumptions:

- (1) The earth is spherical.
- (2) The earth is inertial.
- (3) The orbiter is a point mass. All forces act through this point which is the center of gravity.
- (4) No aerodynamic sideslip occurs in the atmosphere.
- (5) Atmospheric winds rotate with the earth.

It is possible to assume the earth is spherical because the aerodynamic turn is initiated from an equatorial orbit. Final state inclination is still nearly equatorial and the non-spherical effects of the earth are negligible. The earth is treated as inertial since the time spent in the atmosphere during the aerodynamic turn is quite short (approximately 10 min) and the non-inertial effects of the earth would not be a factor in this length of time. It is reasonable to expect that a coordinated turn will be flown during the aerodynamic maneuver so that no moments

will be generated and the orbiter can be approximated as a point source. Similarly, the maneuver will be flown so that the relative velocity vector is nearly along the longitudinal axis of the orbiter in order to keep the heat generated by hypersonic speeds through the atmosphere on the main heat-protective surfaces. Heat generated on the side and top of the orbiter will be kept to a minimum if sideslip is minimized. Finally, the upper atmosphere winds are much too complex to model exactly in a study of this size. However, to treat the winds at altitude as inertial would be too much of a simplification. Accordingly, the main effect of the winds on the shuttle orbit are modelled by assuming the winds to rotate with the earth (Ref 5:12-13).

Lift and Drag Computations

The expressions used to generate $\vec{\text{Lift}}$ and $\vec{\text{Drag}}$ have already been listed in terms of the reference frames. Restated in terms of the state variables, the lift and drag equations are

$$\text{LIFT} = \frac{1}{2}\rho(X,Y,Z)C_L(X,Y,Z,\dot{X},\dot{Y},\dot{Z})V_{rel}^2(X,Y,Z,\dot{X},\dot{Y},\dot{Z})S$$

$$\text{DRAG} = \frac{1}{2}\rho(X,Y,Z)C_D(X,Y,Z,\dot{X},\dot{Y},\dot{Z})V_{rel}^2(X,Y,Z,\dot{X},\dot{Y},\dot{Z})S$$

The reference surface area (S) of the orbiter is a known constant value and the relative velocity can readily be obtained from integration of the equations of motion. However, the values for the atmospheric density (ρ)

and the coefficients of lift and drag (C_L and C_D) will have to be calculated.

The orbiter coefficients of lift and drag are listed in Tables I - IV (Ref 6). These coefficients are a functions of angle of attack (α) and the viscous parameter (VBAR). While angle of attack is directly obtainable, because it will be shown to be a control variable, the VBAR term is a function of the orbiter state.

$$VBAR = M_\infty (C_\infty / Re)^{\frac{1}{2}}$$

where M_∞ = freestream mach number

$C_\infty(T, M_\infty)$ = proportionality factor for linear-viscosity
temperature relationship

$Re(\rho, V_{rel}, S, \text{Kinetic Viscosity})$ = Freestream Reynolds
Number

From the equations listed for Lift, Drag, and VBAR it is apparent that a means of determining the state of the atmosphere is needed.

Model Atmosphere

The model chosen to represent the atmosphere in this study is the 1962 Standard Atmosphere (Ref 11). While a more current version of this model does exist, the 1962 data is used because the Space Shuttle Orbiter Lift and Drag coefficients are based on the 1962 model.

The simplifying assumption that geopotential altitude is equal to geometric altitude is also used here and results in a five to seven percent deviation from the 1962 Standard Atmosphere Model (Ref 5:10). This assumption allows the variation of gravitational acceleration with altitude to be neglected.

With this model, the density, temperature, molecular weight, and viscosity of the atmosphere at any altitude out to 700 km is directly available. These atmospheric parameters are used in the computation of VBAR (Ref 5:22). With VBAR calculated and the angle of attack known, orbiter lift and drag coefficient tables can be entered and C_L and C_D can be determined (Tables I - IV).

A bivariate interpolation scheme is used to determine the values for C_L and C_D when VBAR and angle of attack are between the tabulated values listed in these tables.

For values of VBAR between .01 and .08 the C_L and C_D values in Tables I - IV were determined experimentally, while for VBAR values between .08 and 5.2, C_L and C_D values were determined analytically via the Lockheed Bridging Formula (Appendix A). This formula bridges the transition between free-molecular flow and continuum flow (Ref 5:23).

Table I
Orbiter Lift Coefficients

ALPHA	<u>.010</u>	<u>.020</u>	<u>.040</u>	<u>.060</u>	<u>.080</u>	<u>.310</u>
20.0	.337570	.335040	.321650	.312760	.303860	.261980
25.0	.485270	.483820	.472370	.460870	.4492420	.383570
30.0	.636890	.627990	.614440	.600840	.587290	.497080
35.0	.770820	.758510	.743770	.729030	.714290	.660260
40.0	.884150	.877600	.862240	.846940	.831580	.693920
45.0	.967350	.960750	.945400	.930060	.914710	.762330
50.0	1.021660	1.015560	1.001080	.986680	.972200	.807810

Table II

Orbiter Lift Coefficients - Concluded

VBAR =	<u>.920</u>	<u>1.650</u>	<u>2.500</u>	<u>5.050</u>	<u>.5200</u>
ALPHA					
20.0	.175970	.109500	.078910	.072030	.087310
25.0	.249980	.150510	.106540	.084480	.104420
30.0	.311680	.176790	.117360	.087590	.109390
35.0	.365520	.219910	.123270	.082080	.101440
40.0	.410810	.237990	.120280	.068830	.096830
45.0	.448940	.258310	.127920	.070290	.089940
50.0	.469620	.262590	.123790	.061020	.080150

Table III

Orbiter Drag Coefficients

VBAR =	<u>.010</u>	<u>.020</u>	<u>.040</u>	<u>.060</u>	<u>.080</u>	<u>.310</u>
ALPHA						
20.0	.190800	.207570	.232000	.256430	.280870	.477820
25.0	.299500	.316860	.341420	.366070	.390630	.606860
30.0	.446700	.458290	.481760	.505320	.528790	.758220
35.0	.624700	.631590	.652640	.673690	.694740	.930470
40.0	.834100	.842920	.861230	.879460	.897770	1.130280
45.0	1.066900	1.075010	1.090360	1.105700	1.121050	1.346820
50.0	1.327700	1.334140	1.346280	1.348370	1.370520	1.580650

Table IV
Orbiter Drag Coefficients - Concluded

VBAR =	<u>.920</u>	<u>1.650</u>	<u>2.500</u>	<u>5.050</u>	<u>5.200</u>
ALPHA					
20.0	.882830	1.157240	1.273170	1.372190	1.393070
25.0	1.052340	1.344690	1.480870	1.588750	1.606330
30.0	1.230150	1.545790	1.682720	1.800290	1.827540
35.0	1.415310	1.704850	1.878780	2.001070	2.029030
40.0	1.608470	1.891120	2.062830	2.186220	2.223940
45.0	1.811110	2.083910	2.248670	2.372060	2.406000
50.0	2.012720	2.267240,	2.415300	2.534810	2.571760

Summary

The orbiter system dynamics are represented by differential equations which form the equations of motion. Integration of the equations of motion along the orbit allows the determination of the shuttle state at each integration time step. With the state of the shuttle known, the model atmosphere is used to determine the atmospheric parameters required for calculation of orbiter lift and drag. Lift and drag values are then used in generating an updated orbiter state.

The orbiter state is expressed in terms of eight variables; X , Y , Z , \dot{X} , \dot{Y} , \dot{Z} , ϕ , α . Since the equations of motion are six first-order differential equations and there are eight unknowns, two of the unknown values are controlled. For this study, angle of attack (α) and angle of bank (ϕ) are the controlled values. The resulting solution of the system state is then checked and changes are made to the controlled values which result in an improved state. This process is repeated through an optimization routine which generates final values for the two variables that result in the "best" system state.

III. Optimization Technique

Background

The purpose of this thesis is to find the angle of attack and bank angle histories which obtain the maximum orbit inclination change during an aerodynamic turn maneuver. Since the initial state of the orbiter and functions of the final state are prescribed, and the orbiter is constrained by the equations of motion, this problem can be treated as a classical optimal control problem where the goal is to minimize the performance index, I . A description of the elements of the optimal control problem as it applies to the aerodynamic turn maneuver follows.

Optimal Control

In the aerodynamic turn maneuver the performance index to be minimized is negative inclination change ($-\Delta i$). Therefore, the problem is a maximization problem. To calculate the inclination change, the angular momentum vector of the final state (\vec{H}_f) is compared to the angular momentum vector of the initial state (\vec{H}_i). These vectors are chosen since they involve the complete orbiter state and are normal to the orbit plane (Fig 2). The inclination change is obtained by determining the change in direction between \vec{H}_f and \vec{H}_i .

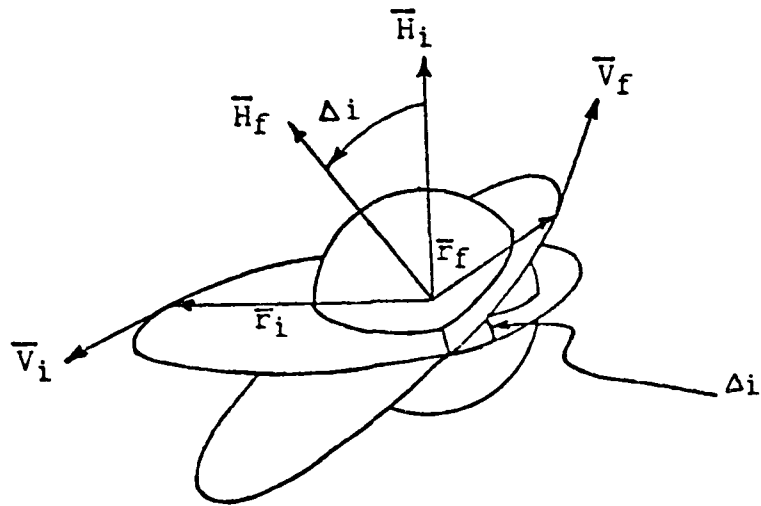


Figure 2. Initial and Final Angular
Momentum Vectors

Since $\vec{H} = \vec{r} \times \vec{v}$

where \vec{r} = orbiter position vector

\vec{v} = orbiter velocity vector

the inner product of \vec{H}_f and \vec{H}_i gives the expression for the change in inclination:

$$\Delta i = \cos^{-1} \frac{(\vec{r}_f \times \vec{v}_f) \cdot (\vec{r}_f \times \vec{v}_f)}{|\vec{r}_f \times \vec{v}_f| |\vec{r}_f \times \vec{v}_f|}$$

where $|\vec{r} \times \vec{v}|$ is the scalar magnitude of the vector cross product.

The initial position and velocity of the orbiter is specified in terms of the state variables. The shuttle proceeds from these initial conditions to a specified set of end conditions while maximizing the inclination change. The time required to complete this maneuver, t_f , is unspecified. For this problem the specified end conditions, M , are altitude and velocity at t_f . The final altitude is to equal the initial altitude and final velocity is to equal initial velocity minus an acceptable velocity loss due to air drag (Δv). Since the orbiter is a dynamic system, it is subject to orbit constraints which are the equations of motion listed in Chapter II. Also, the shuttle is subject to the control constraints that limit angle of attack ($20^\circ \leq \alpha \leq 50^\circ$) and bank angle ($0^\circ \leq \phi \leq 180^\circ$).

Suboptimal Control

The optimal control problem as outlined above is reduced to a suboptimal control problem by approximating

the control variables by a functional form which involves a number of unknown parameters (Ref 8). Suboptimal control is chosen in preference to optimal control because the algorithm to solve the optimal control problem requires controls to be specified as a function of time. The time span of the aerodynamic turn could, therefore, generate large control vectors. In addition, the values to be guessed in the optimal control algorithm do not have a physical significance. In the suboptimal approach, there is not only a very small number of control coefficients to be guessed, but they also have a physical relevance which makes the initial guesses much easier to generate. For this analysis, angle of attack and bank angle are

$$\alpha = \sum_{i=0}^m b_i C_i$$

$$\phi = \sum_{i=0}^n c_i C_i$$

where b_i and c_i are the unknown parameters and C_i is the functional form. Chebyshev polynomials are chosen as the functional form because they are orthogonal. This prevents the matrices used by the optimization scheme from becoming singular due to possible linear dependence of the polynomials. To simplify the problem, the Chebyshev polynomials should be defined over a constant interval. Through the use of Long's transformation, the free final time problem is transformed into a fixed final time problem. Long's

transformation defines a non-dimensional time

$$\tau = t/t$$

where the range of τ is $[0,1]$. The Chebyshev polynomial may then be defined over the interval $[0,1]$. The final time (t_f) is now another unknown parameter of the problem. Thus, the vector of unknown parameters, a , is

$$a = \begin{bmatrix} t_f \\ b_i \\ c_i \end{bmatrix}$$

Since the problem is now treated suboptimally, one objective is to select the correct number of controls, m and n , that accurately approximate the optimal controls. If the order of the control polynomials is too small, the results will not accurately represent the optimal controls. On the other hand, if too high an order control polynomial is selected, the small gain in the performance index will not warrant the large increase in computer time required to obtain the converged solution. The order of the control polynomial representing the angle of attack need not necessarily equal the order of the control polynomial representing the bank angle.

Second-Order Parameter Optimization

The optimal control problem may now be restated as a parameter optimization problem, where the performance index, the end condition constraints, the control variable inequality constraints, and the differential constraints all depend on only the unknown parameters. The solution

to this problem may be found by forming the augmented performance index, F,

$$F(a, v) = I(a) + v^T M(a)$$

where v is the vector of constant Lagrange multipliers.

The conditions to be satisfied by an extremal point are

$$F_a^T(a, v) = 0 \text{ and } M(a) = 0.$$

The values of the parameters and the Lagrange multipliers are now guessed. Unless the guess is the extremal value, it will be observed that

$$F_a^T \neq 0 \text{ and } M \neq 0.$$

In order to drive F_a^T and M to zero, these quantities are then linearized about the guessed values of a and v, so that

$$\delta F_a^T = F_{aa} \delta a + M_a^T \delta v \quad \text{and} \quad \delta M = M_a \delta a$$

where

a is a p x 1 vector of parameters

F_a is a 1 x p vector of 1st partial derivatives

F_{aa} is a p x p matrix of 2nd partial derivatives

M_a is a m x p matrix of 1st partial derivatives

$\delta()$ is the variation of () such that $\delta() = ()_{\text{new}} - ()_{\text{old}}$.

Since we desire $(F_a^T \text{ or } M)_{\text{new}} = 0$, the following relations are valid

$$\delta F_a^T = -P F_a^T \quad \text{and} \quad \delta M = -Q M$$

where Q and P are weighting factors which control the end condition satisfaction and optimization, respectively.

The expressions for δa and δv can now be generated so that

$$\delta a = -F_{aa}^{-1}(PF_a^T + M_a^T \delta v)$$

$$\delta v = (M_a F_{aa}^{-1} M_a^T)^{-1} (-PM_a F_{aa}^{-1} F_a^T + QM).$$

Rather than guessing an initial value for v , it can be computed using the gradient technique with F_{aa} set equal to the identity matrix and δa set equal to zero; then

$$v = (M_a M_a^T)^{-1} ((Q/P)M - M_a I_a^T).$$

If it is desired to use a gradient technique to compute the changes in a , those changes are given by

$$\delta a = -P(F_a^T)$$

Any reasonable value for the control coefficients can be guessed as long as the guess conforms to the control constraints. However, in the next chapter an approach to guessing accurate values for the coefficients will be explained.

IV. Optimization Starting Values

Previous research (Ref 5) indicated the atmospheric turn maneuver is profitable only at perigee altitudes of 85 km and below. Table V lists the orbit inclination changes which resulted from using a 60° angle of bank at various perigee altitudes.

Table V

Inclination Changes Obtained From Previous Research

85 km	80 km	75 km	70 km *
.22 $^\circ$.43 $^\circ$.55 $^\circ$.78 $^\circ$

* The 70 km perigee orbit uses a bank angle of 50° .

The bank angle of 60° was chosen initially since it results in the most inclination change without allowing the maneuver to become a total reentry that will not leave the atmosphere.

Only perigee altitudes of 80 km are considered in this study. This choice is made since inclination changes achieved in an orbit with a perigee higher than 80 km are extremely small and the viscous parameter, VBAR, was often less than 0.01 at perigee altitudes of 75 km and less. The orbiter lift and drag coefficient data available is limited to a VBAR greater than or equal to 0.01.

Orbit Selection

Once a perigee altitude is established, the selection of an apogee altitude will allow the determination of the orbital elements. Since the orbit used in the previous study is not specified, three different orbits are used here. A low apogee of 300 km, a medium apogee of 500 km and a high apogee of 650 km are used. The high apogee is selected to remain below the hazard posed to manned flights by the Van Allen radiation fields. All orbits are considered initially to be direct equatorial.

The three orbits used in this study are initially at a zero degree inclination and have an 80 km perigee. The mean earth radius used for computations is 6378.135 km. The Earth gravitational parameter (μ) used for this study is $3.986012 \times 10^5 \text{ km}^3/\text{sec}^2$. The following two-body relationships are used to calculate the necessary orbital elements for each of the three reference orbits and assume no air drag by the atmosphere:

$$e = 1 - \frac{r_p}{a}$$

$$p = a(1 - e^2)$$

$$v = \left(\sqrt{\frac{\mu}{p}} (1 + e \cos v) \right) \cos v$$

$$TP = \frac{2\pi}{\sqrt{\mu}} a^{3/2}$$

$$e = - \frac{\mu}{2a}$$

The results of these calculations are listed in Table VI.

Table VI

Reference Orbit Elements

ORBIT	80/300	80/500	80/650
e	.0167675242	.0314734553	.0422460329
p	6566.293 km	6661.395 km	6730.966 km
v_o^*	7.6608 km/sec	7.4920 km/sec	7.3703 km/sec
TP	88.29 min	90.31 min	91.84 min
ϵ	-30.344	-29.889	-29.556

* Velocity listed is at apogee ($v=180^\circ$)

Initial Position and Velocity Selection

There is enough information available now to initialize the optimization routine with the position and velocity of the orbiter at apogee and integrate the entire orbit. However, it is assumed that significant orbit plane change will occur only in atmosphere of a certain density. Plane change above this altitude will be negligible. From a study of the 1962 Standard Atmospheric model (Ref 11), an altitude of 100 km above the earth's surface and below is assumed as the level of sufficient density for measurable plane change. The orbiter is inside the atmosphere, as defined here, for approximately 10 minutes per orbit. It is therefore desirable to pick a starting position and velocity for each reference orbit that is just above the 100 km altitude. This will reduce the amount of computer time needed each iteration by neglecting that portion of the orbit in which no appreciable plane change occurs. To determine this starting position and velocity, the integration routine is run from apogee with angle of bank and angle of attack set to zero and the time parameter set to the period of the orbit. Integration by this method gives the position and velocity vector for each time step and from this a height above the Earth is easily calculated. Integration of the orbit in this manner results in a perigee one to two kilometers lower than that calculated using the two-body problem assuming no air drag. These results are still valid, however, since integration using angles of

attack and bank not equal to zero results in a shuttle perigee between 79 and 82 kilometers, depending on the orbit.

From these integrations of the orbit, initial position and velocity vectors are chosen. These vectors are listed in Table VII. The position and velocity vectors become the two constraints for the optimization routine. The program is designed to return the shuttle to the starting height on the other side of perigee and to the scalar value of the starting velocity minus a specified, acceptable velocity loss due to air drag.

Control Coefficient Selection

It is now necessary to initialize the optimization routine with values for the time, angle of attack, and angle of bank control parameters. The optimization routine is designed with weighting factors that determine the priority the routine places on either achieving the end constraints or optimizing the plane change. Initially, emphasis is placed in meeting the end constraints until they are very close to the specified values. At that time, the optimization weighting function, which has been kept small, is slowly increased. In order to minimize the computer time necessary to meet the end conditions, the control parameters which get the final states closest to the end conditions are chosen to be the initial guess.

Table VII

Initial Position and Velocity in Inertial Frame*

INITIAL POSITION

ORBIT	80/300	-3103.9951 \hat{i}	5724.3016 \hat{j}
	80/500	-3238.5651 \hat{i}	5680.0536 \hat{j}
	80/650	-4606.8106 \hat{i}	4636.5561 \hat{j}

INITIAL VELOCITY

ORBIT	80/300	-6.8503 \hat{i}	-3.8470 \hat{j}
	80/500	-6.7306 \hat{i}	-4.0819 \hat{j}
	80/650	-5.7871 \hat{i}	-5.4225 \hat{j}

* All position and velocity vectors are initially equatorial and have no \hat{k} components.

To find the best starting parameters, over 150 integration runs were made for a single orbit with various angles of attack and bank angle values. This allows a determination of how well various combinations of the control parameters meet the constraints. A listing of the pertinent results from these runs for the 80/300, 80/500, 80/650 orbits is listed in Tables VIII, IX, and X respectively.

The first value listed in Tables VIII, IX, and X. is the difference between the starting and the final altitude at the end of integration. A positive value means the shuttle finished higher than the initial altitude. The second value in the tables is the difference in initial velocity loss for the maneuver. In this case, the allowable velocity loss is 60 mps. Positive velocity values mean the orbiter lost less than 60 mps during the orbit. A negative value means the orbiter lost not only the 60 mps, but also the additional listed velocity. The third value in the tables is the inclination change that results from those control parameters. With this data, the "best" possible control parameters can be chosen that will initially allow the optimization routine to not only come closest to the desired end conditions, but also give the largest possible inclination change.

Table VIII

End Condition Miss Errors 80/300 Orbit

		ANGLE OF ATTACK				
		20°	25°	30°		
ANGLE OF BANK	0°	ALT MISS	-1.17	-7.19	-19.27	km
		VEL MISS	.008	.004	.003	kps
		Δi	0.	0.	0.	deg
	5°	ALT MISS	-1.36	-7.59	-20.02	km
		VEL MISS	.008	.005	.003	kps
		Δi	.04	.06	.18	deg
	10°	ALT MISS	-2.28	-8.47	-20.86	km
		VEL MISS	.008	.005	.003	kps
		Δi	.10	.11	.20	deg
	15°	ALT MISS	-3.57	-10.21	-22.91	km
		VEL MISS	.009	.005	.003	kps
		Δi	.15	.17	.22	deg
20°	ALT MISS	-5.66	-12.66	-26.04	km	
	VEL MISS	.010	.006	.002	kps	
	Δi	.20	.24	.28	deg	

$$\Delta v = 60 \text{ mps}$$

Table IX

End Condition Miss Errors 80/500 Orbit

		ANGLE OF ATTACK			
		20°	25°	30°	
0°	ALT MISS	32.7	29.3	22.5	km
	VEL MISS	-.011	-.016	-.018	kps
	Δi	0.	0.	0.	deg
5°	ALT MISS	31.9	29.9	22.7	km
	VEL MISS	-.010	-.016	-.018	kps
	Δi	.03	.04	.04	deg
10°	ALT MISS	31.4	29.1	21.9	km
	VEL MISS	-.010	-.015	-.018	kps
	Δi	.06	.07	.09	deg
15°	ALT MISS	31.6	27.1	19.5	km
	VEL MISS	-.010	-.015	-.017	kps
	Δi	.08	.11	.13	deg
20°	ALT MISS	30.2	26.6	18.0	km
	VEL MISS	-.009	-.014	-.016	kps
	Δi	.11	.14	.17	deg

$\Delta v = 60$ mps

ANGLE
OF
BANK

Table X

End Condition Miss Errors 80/650 Orbit

		ANGLE OF ATTACK				
		20°	25°	30°		
ANGLE OF BANK	0°	ALT MISS	159.7	152.5	140.8	km
		VEL MISS	-.164	-.166	-.163	kps
		Δi	0.	0.	0.	deg
	5°	ALT MISS	161.1	152.6	141.0	km
		VEL MISS	-.164	-.166	-.163	kps
		Δi	.03	.04	.05	deg
	10°	ALT MISS	161.1	153.2	139.9	km
		VEL MISS	-.164	-.165	-.162	kps
		Δi	.07	.09	.10	deg
	15°	ALT MISS	157.8	149.7	136.3	km
		VEL MISS	-.163	-.164	-.161	kps
		Δi	.10	.13	.15	deg
20°	ALT MISS	156.6	147.6	134.9	km	
	VEL MISS	-.163	-.163	-.159	kps	
	Δi	.14	.17	.20	deg	

$\Delta v = 60$ mps

V. Results and Conclusions

Optimization Analysis

A second-order technique to generate updated control coefficients is preferred to a gradient technique because of faster convergence. In the suboptimal approach to the aerodynamic turn maneuver that was outlined in Chapter III, the second-order parameter method requires the computation of the F_{aa} matrix, a second derivative matrix, by numerical means. The numerical approach to solving for F_{aa} is chosen over an analytical approach because it requires considerably less computer time. However, numerical differentiation does require perturbations in the quantities the derivative is taken with respect to. For example, numerical computation of F_{aa} requires perturbation of the a's.

Early in the control parameter optimization search, problems were encountered with the second derivatives. The values of the elements of the F_{aa} matrix were found to be changing erratically by a power of ten. Since the size of the perturbations of the a's affect the behavior of the F_{aa} matrix, a parametric study using different size perturbations was conducted to determine whether or not the erratic behavior of the F_{aa} matrix could be corrected.

After evaluating the effects of various size perturbations on the F_{aa} matrix, it was determined that continued

efforts to optimize using the second-order parameter method would fail to produce a sequence of control histories which would ultimately converge. A switch to the gradient technique was made at this time to see if the optimization routine would move in a consistent direction toward convergence.

While the gradient technique did continually move toward an optimum control history and improve both the end conditions and inclination change, it was very costly in terms of computer time. The results listed in this chapter required over 32000 CP seconds of computer time to generate. In retrospect, it would have been faster in both my time and computer time to use another second-order method rather than continue with the gradient technique for as long as was ultimately required for convergence. Any additional research on the aerodynamic turn maneuver should utilize a second-order method such as the Davidson-Fletcher-Powell variable metric technique. If continued use of a gradient method is desired, use of the Fletcher-Reeves conjugate gradient technique would speed up convergence time.

Apogee Analysis

Before deciding to concentrate this study on orbits with an 80 km perigee a feasibility study of other orbits was undertaken. The results of Harding's research indicated orbits between 70 and 85 km perigees were profitable for the aerodynamic turn maneuver. However, initial runs

at 70 to 75 km perigee altitudes ran into difficulty when the viscous parameter, VBAR, fell below the .01 value which was the limit of orbiter aerodynamic coefficients of lift and drag. Inclination changes at perigees of 85 km and above were insignificant since atmospheric density at these altitudes is too low for an effective aerodynamic maneuver. While it would be possible to compute lift and drag coefficients for perigee altitudes below 70 km, extended operations at these low altitudes are unrealistic because of the heating effects on the orbiter at hypersonic velocities. This tends to indicate the aerodynamic turn maneuver, while feasible, has a limited range of perigee altitudes that produce significant orbit inclination changes.

Comparison of the aerodynamic turn maneuver to the pure rocket burn is a purpose of this study. For a circular orbit, the inclination change (Δi) generated by a rocket burn of a specific change in velocity (Δv) is:

$$\arcsin \frac{\Delta i}{2} = \Delta v / 2v$$

The value used for v is the scalar velocity at apogee. Apogee is chosen since there the shuttle will have the lowest velocity and the largest Δi will be obtained for a specified velocity change component perpendicular to the plane of the orbit. Although the formula list above is for a circular orbit, the resulting Δi computed still

provides a good comparison value since the shuttle orbit is nearly circular.

The resulting Δi for a given Δv using a rocket burn is listed in Table XI .

Table XI

Inclination Change
Using Rocket Motor

Δv (mps)	40	50	60	80	100	300
Δi (deg)	.286	.358	.429	.572	.716	2.15

The maximum orbit plane change obtained by the optimized controls in the aerodynamic turn maneuver for the three reference orbits with a Δv of 60 mps is listed in Table XII.

Table XII

Maximum Orbit Plane Change ($\Delta v=60$ mps)

	ORBIT		
	80/300	80/500	80/650
Δi (deg)	.04	.44	.71

It is apparent that the 80/300 orbit accomplishes almost no inclination change. When compared to the rocket burn results listed in Table XI , the 80/500 orbit is successful in achieving more inclination change while the 80/650 orbit betters the rocket burn by 65%. The implications here are

that as the reference orbit gets more elliptical the aerodynamic turn maneuver is more profitable. Why this occurs can be explained by comparing the velocity histories of the reference orbits inside the atmosphere. As the orbit becomes more elliptical the velocity of the shuttle increases in the portion of the orbit near perigee. The velocity of the shuttle at perigee is listed in Table XIII for the reference orbits.

Table XIII

Velocity of Orbiter at Perigee

PERIGEE VELOCITY (KPS)	ORBIT		
	80/300	80/500	80/650
	7.88	7.97	8.00

While this has the effect of raising freestream Mach number, it causes a reduction in the value computed for the viscosity parameter (VBAR). Table XIV lists the time spent inside the atmosphere for each reference orbit. The effect of the higher velocities in the more elliptical orbits is quite apparent in the reduced time the more elliptical orbit allows the shuttle to stay in the atmosphere.

Table XIV

Time Inside Atmosphere

TIME (sec)	80/300	80/500	80/650
		931	621

To understand why the smaller VBAR values result in larger inclination changes it is necessary to look at the VBAR values calculated for the orbiter. Table XV lists the VBAR history for each reference orbit for the portion of the orbit between entry into the atmosphere and perigee. The VBAR history is mirrored for the portion of the orbit from perigee until it departs the atmosphere.

Table XV
VBAR History in Atmosphere ($\Delta v=60$ mps)

		VBAR		
Altitude (km)	100	.232	.098	.097
	95	.095	.094	.093
	90	.090	.086	.075
	85	.062	.062	.059
	80	.047	.045	.038
		80/300	80/500	80/650

By calculating the L/D ratios for the VBAR's listed in Table XV, a comparison can be made of the efficiency of each orbit. These L/D ratios are listed in Table XVI.

Table XVI
L/D Ratios Inside Atmosphere ($\Delta v=60$ mps)

		L/D RATIO ($\alpha=25^\circ$)		
		80/300	80/500	80/650
ALTITUDE (km)	100	.761	1.10	1.09
	90	1.12	1.13	1.18
	80	1.35	1.38	1.40

The L/D ratios in Table XVI indicate that as the orbiter enters the atmosphere at a higher velocity because of a more elliptical orbit, the aerodynamic turn maneuver is more efficient. The more efficient maneuver obtains more inclination than the less efficient maneuver for the same specified velocity loss.

At this point, it is desirable to look at the results of changing the acceptable velocity loss per orbit. A velocity loss of 300 mps is considered to be the maximum acceptable Δv loss in an aerodynamic turn maneuver. This figure is used since that is the maximum Δv the orbiter rocket motor can produce using internal fuel.

The inclination changes listed in Table XI which were obtained using only the rocket motor show that Δi is a linear function of Δv for all values of Δv considered in this problem. Based on these results it appears that accepting a larger Δv loss per orbit during the aerodynamic turn maneuver would give a larger Δi proportional to the increase in Δv .

Table XVII indicates this did not occur. In fact the lower velocity loss returned a proportionally higher Δi .

Table XVII

Inclination Change for Various Velocity Losses (80/500 orbit)

	VELOCITY LOSS (mps)			
	30	40	50	60
$\Delta i(\text{deg})$.27	.35	.37	.44

These results show that Δi is not a linear function of Δv for the aerodynamic turn maneuver.

When the optimization routine is constrained to lose a larger velocity per orbit, there are essentially two ways to do this. One, the orbiter can descend to a lower altitude and stay longer in the atmosphere. Since the program used here specified the orbit to be optimized, this option was not available. The second method which could be used is to increase the angle of attack. What must be analyzed here is the effect of constraints in the optimization routine. Because the optimization problem is set up to obtain the maximum Δi for a given Δv , the program makes no effort to find the most efficient L/D ratio for each orbit. The optimum control history for each orbit will be applicable for a specific velocity loss. However, there may be another velocity loss which will produce the most efficient Δi in terms of Δv expended to obtain the inclination change. Thus, the lower specified velocity loss returned a larger Δi on a percentage basis. To understand why this occurs it is necessary to calculate the L/D ratios at various angles of attack. The L/D ratios for different angles of attack at perigee VBAR are listed in Table XVIII.

Table XVIII

L/D Ratios versus Angle of Attack (Perigee VBAR)

		L/D RATIOS		
		80/300	80/500	80/650
Angle of Attack (deg)	20°	1.21	1.30	1.39
	30°	1.19	1.23	1.275
	40°	.963	.982	1.00
	50°	.726	.732	.744

Table XVIII shows that as angle of attack increases above 20° the orbiter L/D ratio becomes less efficient. Aerodynamic lift and drag coefficients are available only for angles of attack between 20° and 50°. Thus, the most efficient aerodynamic turn maneuver for any orbit in terms of L/D ratios would seek to maximize Δi for Δv which called for an angle of attack of 20°. The optimization problem can be changed slightly so that angle of attack is constrained to remain at 20°. Various acceptable Δv 's could be tried until an optimum control history for angle of bank is determined that maximizes inclination change.

The inclination change which this procedure would generate is going to be small (approximately .20°). However, this inclination change will be the largest one possible for the most efficient orbiter L/D ratio. The orbiter can now utilize this optimum control history over

several orbits until the desired orbit plane change is obtained. Using this approach until the total Δv of the orbits reaches the 300 maximum allowed, a large total Δi is possible. This technique on the 80/500 orbit produces a total inclination change of 3° while the 80/650 orbit achieves a 4° inclination change. Thus, the Δi obtained by the aerodynamic turn maneuver exceeds the inclination change of 2.15° generated by the rocket burn (Table XI) by 40% on the 80/500 orbit and by 86% on the 80/650 orbit.

Higher-Order Control Analysis

The optimization program was started with the "best guess" of the controls coefficients as explained in Chapter IV . The control coefficients were initially constant values. The program was allowed to optimize until the increases in inclination change were insignificant. Controls were then increased to three parameters for both the angle of attack and angle of bank and the process repeated.

This procedure was accomplished again for five, seven, and nine control parameters for only the angle of bank. Higher order controls for the angle of attack did not prove necessary since angle of attack essentially remained constant between 21° - 24° depending on the reference orbit.

The increases in control parameters for the angle of bank proved beneficial with each increase raising the inclination change obtained. This occurred through seven control parameters for the angle of bank. Beyond seven

parameters, there was no appreciable increase in inclination change. The plots of control history and inclination change are listed in Figures 3,4,5, and 6. The increase in Δi as the control parameters increased from one to seven is approximately $.11^\circ$. This indicates a nearly 30% improvement in inclination change can be gained from the use of higher order controls rather than a constant bank angle.

The control history for the seven bank angle parameters indicates a converged solution. The oscillations in the bank angle history for that portion of the turn inside the atmosphere ($.3 < \text{Time} < .6$) have damped out. Further increases in the number of bank angle parameters had little effect on the control history.

An analysis of the control history indicates the converged solution commands the shuttle to roll inverted, $\phi = 180^\circ$, as the atmosphere is approached. This will orient the lift vector to aid in reaching perigee. The bank angle is slowly reduced until the atmosphere is reached with $\phi = 60^\circ$, ($\text{TIME} = .3$). Most of the inclination change occurs between $.3 < \text{TIME} < .6$, where the bank angle slowly decreases from 80° to 60° . As the atmosphere is departed ($\text{TIME} = .6$), the lift vector is oriented up ($\phi = 0^\circ$) to assist in returning to the specified final altitude. Flying this control schedule is easily within the capabilities of the orbiter's computer.

This study has shown that the aerodynamic turn maneuver is profitable for the Space Shuttle Orbiter and a flyable control history does result from the use of higher order controls and optimization. However, the small inclination changes available from the maneuver and the low perigee, high eccentricity orbits which must be used to get meaningful inclination changes, severely limit the usefulness of this maneuver. Additional research on this subject is not recommended.

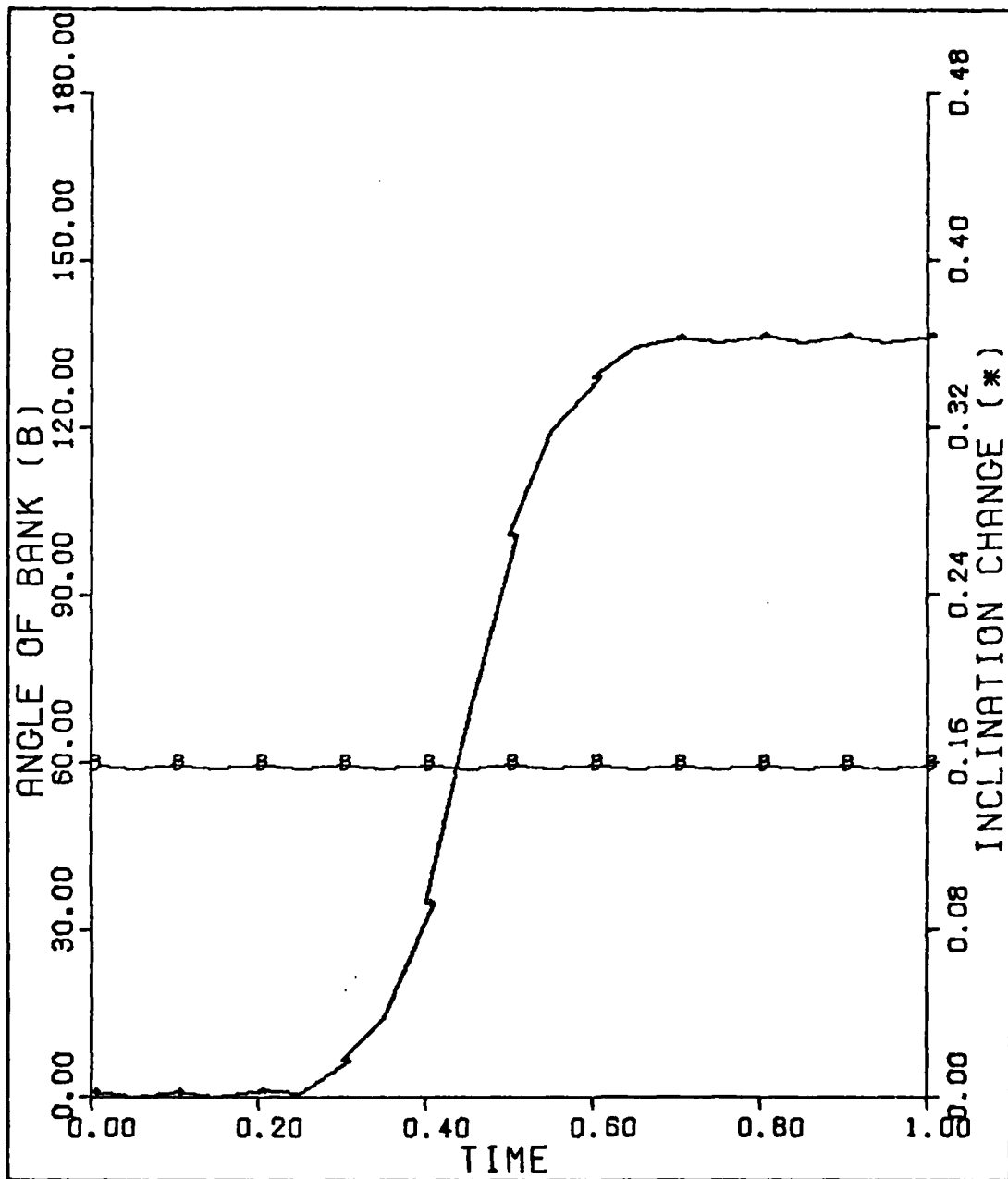


Figure 3. Control History- One Control Parameter

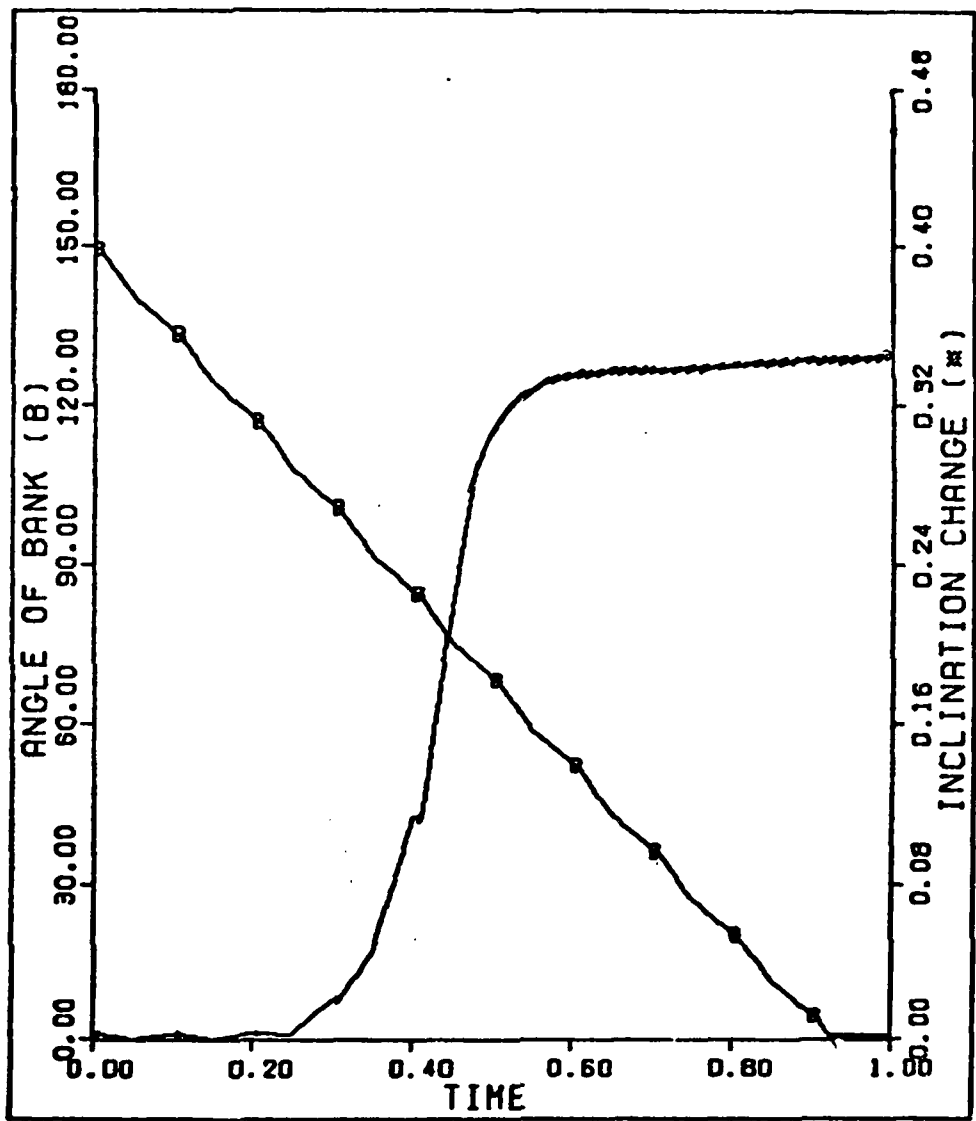


Figure 4. Control History-Three Control Parameters

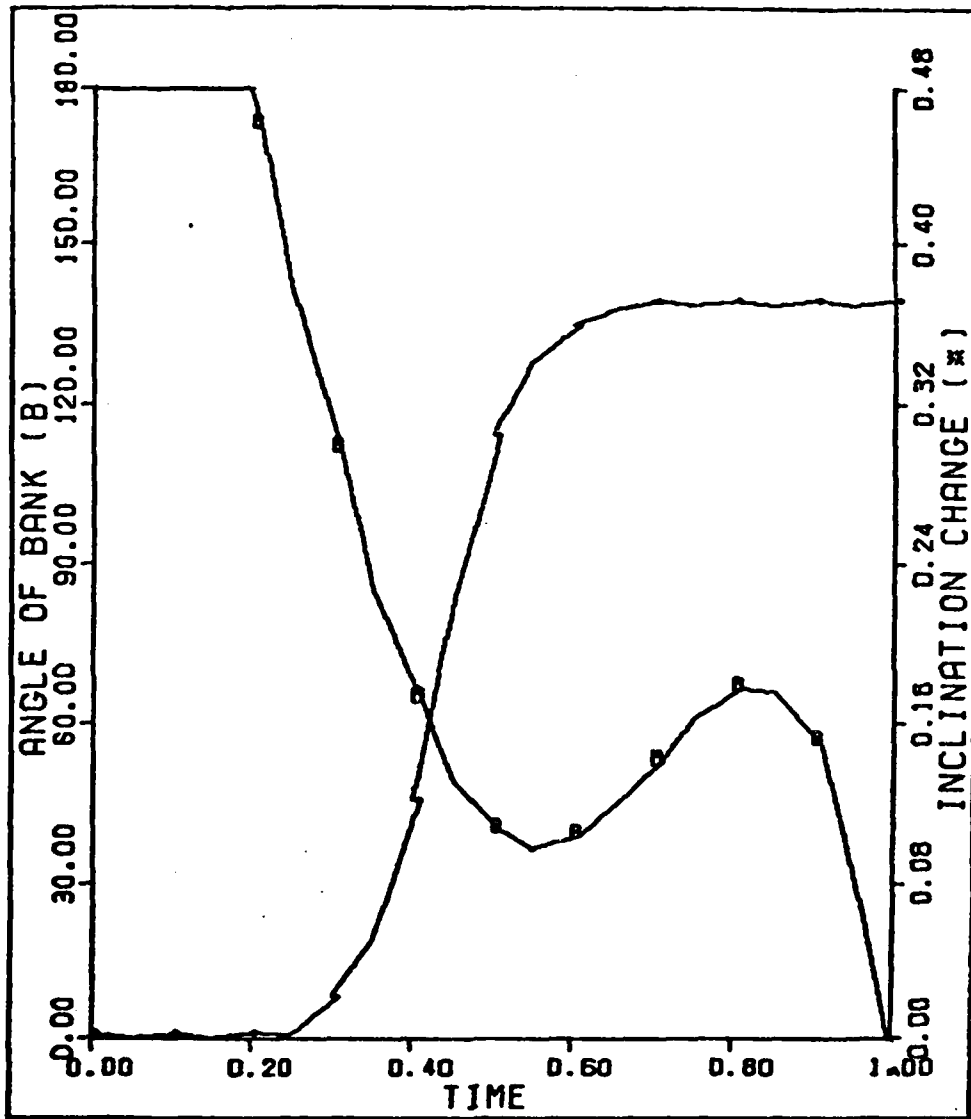


Figure 5. Control History- Five Control Parameters

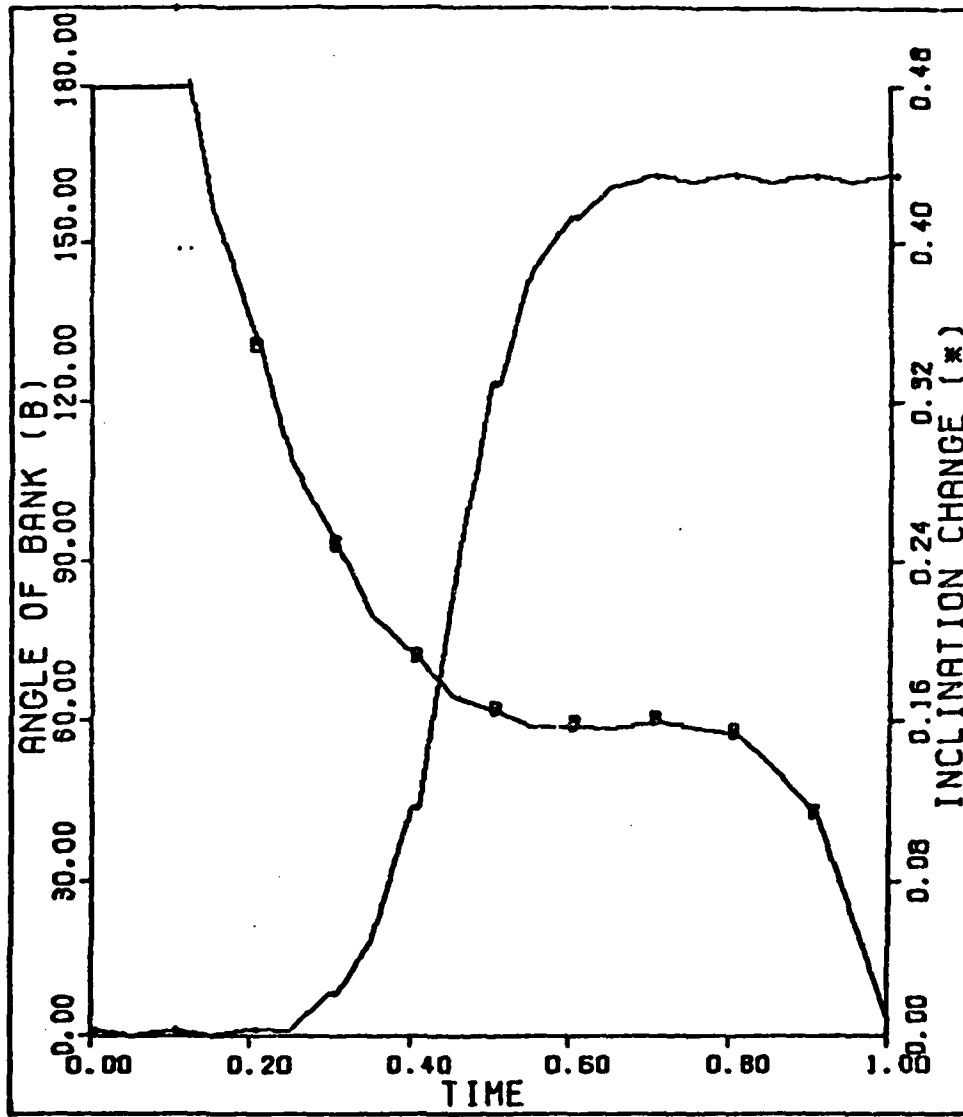


Figure 6. Control History- Seven Control Parameters

Bibliography

1. Abramowitz, Milton and I. Segun. Handbook of Mathematical Functions. New York: Dover Publishing, Inc., 1964.
2. Bate, Roger, D. Mueller and J. White. Fundamentals of Astrodynamics. New York: Dover Publishing, Inc., 1971.
3. Citron, Stephen. Elements of Optimal Control. New York: Holt, Rinehart and Winston, Inc., 1969.
4. Fox, Richard L. Optimization Methods For Engineering Design. Reading, Massachusetts: Addison-Wesley Publishing Company, 1971.
5. Harding, Roger R., "Optimum Orbit Plane Change Using A Skip Reentry Trajectory For The Space Shuttle Orbiter," MS Thesis, AF Institute of Technology, Dayton, OH, December, 1978.
6. Hill, Oliver. Orbiter Aerodynamic Data. Houston: 1978.
7. Hull, David. "Application of Parameter Optimization Methods to Trajectory Optimization," American Institute of Aeronautics and Astronautics, 74-825: 1974.
8. Hull, David and L. Edgeman. "Suboptimal Control Using a Second-Order Parameter Optimization Method," Journal of Optimization Theory and Applications, 17:481-490: 1975.
9. Kuethé, A. and J. Schetzer. Foundations of Aerodynamics. New York: John Wiley and Sons, Inc., 1959.
10. National Aeronautics and Space Administration. Space Shuttle. Houston, 1975.
11. National Aeronautics and Space Administration, United States Air Force, United States Weather Bureau. U.S. Standard Atmosphere, 1962. Washington: U.S. Government Printing Office, 1962.
12. National Oceanic and Atmospheric Administration, National Aeronautics and Space Administration, United States Air Force, U.S. Standard Atmosphere, 1976. Washington: U.S. Government Printing Office, 1976.

APPENDIX A

Lockheed Bridging Formula*

*(Ref 5:53)

The Lockheed Bridging Formula is used to evaluate the aerodynamic force coefficients for the Space Shuttle Orbiter. The formula bridges the transitional flow regime from continuum flow to free-molecular flow. The formula is:

$$C_{\text{trans}} = C_{\text{cont}} + (C_{\text{F.M.}} - C_{\text{cont}}) \sin^n(\pi(A + B \log_{10} K_n))$$

where

C_{cont} = viscous force coefficient values at $V_{\text{BAR}} = 0.08$

$C_{\text{F.M.}}$ = viscous force coefficient values at $V_{\text{BAR}} = 5.2$
(free-molecular flow)

$$n = 2$$

$$A = 3/8$$

$$B = 1/8$$

$$K_n = \text{Knudsen number} = \lambda/L_{\text{ref}}$$

$$L_{\text{ref}} = 12.059 \text{ meters}$$

$$\lambda = \text{mean free path} = RT/P (2N\sigma^2)^{-1}$$

$$R = \text{universal gas constant} = 8.314 \times 10^3 \text{ N-m/kg K}$$

T = temperature

P = pressure

$$N = \text{Avogadro's number} = 6.022 \times 10^{26} \text{ kmol}^{-1}$$

σ = effective molecular collision diameter

$$= 3.65 \times 10^{-10} \text{ meters}$$

APPENDIX B

Optimization Program

The program used to solve the optimization of the orbiter aerodynamic turn maneuver is listed in this appendix. A flow chart is included to show the calling order of the subroutines (Fig 7). The program, as listed here, is set up to solve the optimization problem using the gradient technique. Comments are incorporated into the program to explain the function of the subroutines and define key variables.

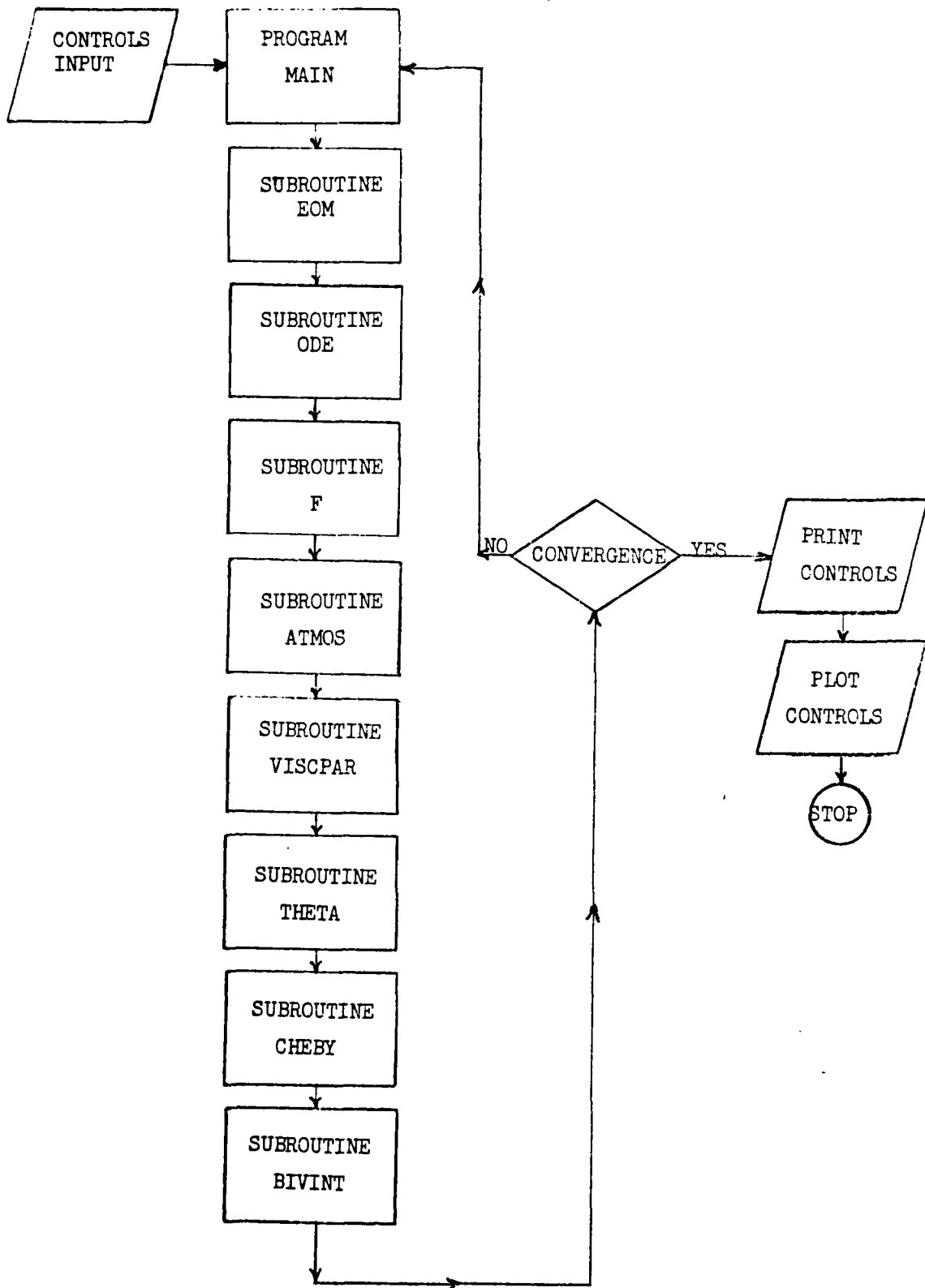


Figure 7, Optimization Program Flowchart

```

C ***** THE PROGRAM MAIN COMPUTES THE PARTIAL
C DERIVATIVES USED IN THE PARAMETER OPTIMIZATION SCHEME.
C A SECOND-ORDER PARAMETER OPTIMIZATION TECHNIQUE IS USED
C BASED ON THE PAPER BY EDGE MAN AND HULL BY THE SAME NAME.
C *****
PROGRAM SHUTTLE(INPUT,OUTPUT,TAPES=INPUT,PLOT)
EXTERNAL F
DIMENSION CDV(8,12),CLV(8,12),ARAY(22,5),7B(6),Y1(6)
DIMENSION XI(6),YP(6),WORK(250),IWORK(5),UNM(2),Y(6)
DIMENSION GB(10),GBB(10,10),FBT(10),FBB(10,10),FBBI(10,10)
DIMENSION DB(10),V(10),Z(10)
DIMENSION XP(6),DBP(10),RG(4),HBHBT(4,4),HBHBTI(4,4)
DIMENSION XPP(6),XP1(6),XP2(6),XP3(6),XP4(6)
DIMENSION HP(2),HPP(2),HP1(2),HP2(2),HP3(2),HP4(2)
DIMENSION H(2),HB(2,10),HBB(2,10,10),E(2,10),
-F1(4,4),FI(4,4),G(2)
DIMENSION RP(2),RQ(2),DC(2),S(10),C(2),FBT(10,2)
DIMENSION DELINC(7)
DIMENSION AOB(50),INKCHG(50),RADIAN(50),ACA(50),TIME(50)
COMMON/B/B(16)
COMMON/BP/BP(16)
COMMON/N/NE,NP,NPP1,NPP2
COMMON U,RHO,VISC,REN,VPAR,PHI,COEFDRG,COEFLFT
COMMON CDV,CLV,ARAY,V1,RA,DT
COMMON NOM
REAL NOM,INKCHG
READ*,(XI(I),I=1,6)
C INITIAL CONDITIONS, XI(1 THRU 3) IS X,Y,Z POSITION
C INITIAL CONDITIONS, XI(4 THRU 6) IS VX,VY,VZ VELOCITY
READ*,((CDV(N,M),N=1,8),M=1,13)
READ*,((CLV(N,M),N=1,8),M=1,13)
READ*,((ARAY(I,J),J=1,5),I=1,22)
C CDV IS THE DRAG COEFFICIENT DATA
C CLV IS THE LIFT COEFFICIENT DATA
C ARAY IS THE ATMOSPHERIC MODEL DATA
C NE=NUMBER OF STATE EQUATIONS
C NP=NUMBER OF PARAMETERS
C NC=NUMBER OF CONSTRAINTS
C NPP1 AND NPP2 ARE THE NUMBER OF CONTROL PARAMETER
C COEFFICIENTS FOR ANGLE OF ATTACK AND BANK, RESPECTIVELY
N=6
NE=6
NP=7
NC=2
NPP1=3
NPP2=3
C C1 AND C2 ARE THE CONSTRAINTS. HERE FINAL ALTITUDE AND VEL.
C1=6538.0

```

```

C2=((XI(4)**2+XI(5)**2+XI(6)**2)**.5)-.06
IT=ITI=1
C   B VALUES ARE COEFFICIENTS OF CONTROL PARAMETERS
B(1)=1941.45654223
B(2)=23.1448603169
B(3)=.00727844740891
B(4)=.0104410966147
B(5)=.932318675716
B(6)=-1.16885024800
B(7)=.00377977989972
C   C'S ARE INITIAL LAMBDA VALUES.
C(1)=.001
C(2)=.001
PCT=0.1
C   DELB IS PERTUBATION STEP SIZE
DELB=1.0E-02
C   DT IS THE TIME STEP SIZE
DT=.6656666E-03
100 CONTINUE
PRINT 90,IT
80  FORMAT(1H,*ITERATION *,I3)
DO 71 I=1,NP
71  BP(I)=B(I)
C   NEXT STATEMENT CONTROLS WHICH ITERATION GETS PLOTTED.
C   PLOT ROUTINE PLOTS A LEFT Y AXIS (ANGLE OF BANK) VEPSJS
C   THE X AXIS (TIME) AND A RIGHT Y AXIS (INCLINATION CHANGE)
C   PLOT IS 6 INCHES HIGH BY 5 INCHES WIDE.
IF(IT.NE.3) GO TO 732
T=0.0
DO 632 N=1,23
INKCHG(N)=ABS(INKCHG(N))
632 CONTINUE
DO 733 N=1,21
CALL T4ETA(T,UNM)
AOB(N)=UNM(2)*57.29577951
TIME(N)=T
T=T+0.05
733 CONTINUE
CALL PLOT(0.,-.5,-3)
CALL PLOT(2.5,2.5,-3)
CALL PLOT(5.,0.,-2)
CALL PLOT(0.,7.,-2)
CALL PLOT(-6.,0.,-2)
CALL PLOT(0.,-7.,-2)
CALL PLOT(.5,.5,-3)
CALL SCALE(TIME,F.,21,1)
CALL SCALE(AOB,5.,21,1)
CALL AXIS(0.,0.,4HTIME,-4,5.,0.0,0.0,.2)

```

```

CALL AXIS(0.,0.,17HANGLE OF BANK (B),17,6.,90.,0.0,30.)
TIME(22)=0.0
TIME(23)=.2
AOB(22)=0.0
AOB(23)=25.
CALL LINE(TIME,AOB,21,1,2,29)
IS=IS-1
CALL SCALE(INKCHG,6.,IS,1)
CALL AXIS(5.,0.,22HINCLINATION CHANGE (*),-22,6.,90.0,
INKCHG(IS+1),INKCHG(IS+2))
CALL LINE(TIME,INKCHG,IS,1,2,17)
CALL PLOTE(N)
GO TO 50
732 PRINT 801,8
801 FORMAT(1X,6E21.12)
DO 12 I=1,NE
12 Y1(I)=XI(I)
NOM=0.3
CALL EOM(T,Y1,DEG,INKCHG,IS,-1.0)
NOM=NOM+1.0
H(1)=(RA-C1)/1000.
H(2)=((Y1(4)**2+Y1(5)**2+Y1(6)**2)**.5)-C2
PRINT*, "H(1) AND H(2) = ",H(1),H(2)
DELINC(1)=-DEG
DO 78 K=1,NP
DO 75 L=1,NP
75 BP(L)=B(L)
DBP(K)=DFLB*BP(K)
IF(ABS(DBP(K)).LE.DELB) DBP(K)=DELB
BP(K)=BP(K)+DBP(K)
DO 13 I=1,NE
13 XP(I)=XI(I)
SP=2.0
CALL EOM(T,XP,DEG,INKCHG,IIP,SP)
HP(1)=RA-C1
HP(2)=((XP(4)**2+XP(5)**2+XP(6)**2)**.5)-C2
DELINC(2)=-DEG
DO 750 L=1,NP
750 BP(L)=B(L)
BP(K)=BP(K)-DBP(K)
DO 14 I=1,NE
14 XPP(I)=XI(I)
CALL EOM(T,XPP,DEG,INKCHG,IIP,SP)
HPP(1)=RA-C1
HPP(2)=((XPP(4)**2+XPP(5)**2+XPP(6)**2)**.5)-C2
DELINC(3)=-DEG
DO 77 L=1,NC
77 ;B(L,K)=(HP(L)-HPP(L))/(2.0*DBP(K))

```

```

GB(K)=(DELINC(2)-DELINC(3))/(2.0*DBP(K))
78 CONTINUE
C THIS SECTION IS THE PARAMETER OPTIMIZATION SCHEME
PRINT*," "
PRINT*,"**** HB MATRIX ****"
PRINT*,((HB(I,M),M=1,NP),I=1,NC)
PRINT*," "
PRINT*,"**** GB VECTOR ****"
PRINT*,(GB(K),K=1,NP)
PRINT*," "
DO 4 I=1,NP
DO 4 J=1,NC
4 HBT(I,J)=HB(J,I)
DO 5 I=1,NC
DO 5 K=1,NC
HBHBT(I,K)=0.0
DO 5 J=1,NP
5 HBHBT(I,K)=HBHBT(I,K)+HB(I,J)*HBT(J,K)
CALL GAUSD(NC,1.0E-30,HBHBT,HBHBTI,KER,4)
DO 666 I=1,NC
RG(I)=0.0
DO 666 J=1,NP
666 RG(I)=RG(I)+HB(I,J)*GB(J)
SS=.0000001
Q=.001
DO 7 I=1,NC
C(I)=0.0
DO 7 J=1,NC
7 C(I)=C(I)+HBHBTI(I,J)*(0*H(J)-RG(J))
11 CONTINUE
PRINT*," "
PRINT*,"**** C VECTOR ****"
PRINT*," "
PRINT*," ",C(1)," ",C(2)
DO 10 I=1,NP
CC=0.0
DO 110 J=1,NC
110 CC=CC+C(J)*HB(J,I)
10 FBT(I)=GB(I)+CC
PRINT*," "
PRINT*,"*****FBT VECTOR *****"
PRINT*," "
PRINT*,(FBT(K),K=1,NP)
DO 549 I=1,NP
DO 549 J=1,NP
FBBI(I,J)=0.0
IF(I.EQ.J) FBBI(I,J)=1.0
549 CONTINUE

```

```

DO 20 I=1,NC
DO 20 K=1,NP
E(I,K)=0.0
DO 20 J=1,NP
20 E(I,K)=E(I,K)+FBBI(J,K)*HE(I,J)
DO 25 I=1,NC
DO 25 K=1,NC
F1(I,K)=0.0
DO 25 J=1,NP
25 F1(I,K)=F1(I,K)+E(I,J)*HBT(J,K)
CALL GAUSS(NC,1.0E-30,F1,FI,KER,4)
DO 30 I=1,NC
G(I)=0.0
DO 30 J=1,NP
30 G(I)=G(I)+E(I,J)*FBT(J)
DO 548 I=1,NC
548 DC(I)=0.0
DO 40 I=1,NP
S(I)=0.0
DO 40 J=1,NC
40 S(I)=S(I)+HBT(I,J)*DC(J)
DO 45 I=1,NP
V(I)=0.0
Z(I)=0.0
DO 45 J=1,NP
V(I)=V(I)+FBBI(I,J)*FBT(J)
Z(I)=Z(I)+FBBI(I,J)*S(J)
45 DB(I)=- (SS*V(I))-Z(I)
DBN=0.0
DO 145 I=1,NP
145 DBN=DBN+DB(I)*DB(I)
DBN=SQRT(DBN)
BN=0.0
DO 255 I=1,NP
BN=BN+B(I)*B(I)
255 CONTINUE
BN=SQRT(BN)
HN=0.0
DO 150 I=1,NC
150 HN=HN+H(I)*H(I)
HN=SQRT(HN)
PRINT*," "
PRINT*,"***** DBN HN *****"
PRINT*," "
PRINT 82,DBN,HN
82 FORMAT(4X,2E20.8,/)
PRINT*," "
PRINT*,"***** DB *****"

```

```

PRINT*, " "
PRINT 83, DB
83  FORMAT(4X, 6E20.8, /)
PRINT*, " "
PRINT*, "**** DC ****"
PRINT*, " "
PRINT 84, DC
84  FORMAT(4X, 3E20.8, ///)
IF((DBN.LT.1.0E-04).AND.(HN.LT.1.0E-03)) GO TO 60
DO 50 I=1, NP
50  B(I)=B(I)+DB(I)
IF(B(2).GT.50.0) B(2)=50.0
IF(B(2).LT.20.0) B(2)=20.0
IF(B(3).LT.-3.14) B(3)=-3.14
IF(B(3).GT.3.14) B(3)=3.14
DO 55 I=1, NC
55  C(I)=C(I)+DC(I)
IT=IT+1
IF(IT.GT.ITI+25) GO TO 60
GO TO 100
60  CONTINUE
PRINT 85
85  FORMAT(2X* CONVERGENCE *)
PRINT 85, 2
86  FORMAT(//, 4X, 6E21.12, //)
STOP
END
C  ****SUBROUTINE GAUSD IS A MATRIX INVERSION ROUTINE****
SUBROUTINE GAUSD(M, EPS, BB, CC, KER, LAY)
DIMENSION BB(LAY, LAY), CC(LAY, LAY), A(20, 20), X(20, 20)
EP=EPS
N=M
DO 100 J=1, N
DO 100 K=1, N
100 A(J, K)=BB(J, K)
DO 1 I=1, N
DO 1 J=1, N
1 X(I, J)=0.0
DO 2 K=1, N
2 X(K, K)=1.0
DO 34 L=1, N
KP=J
Z=0.0
DO 12 K=L, N
IF(Z-ABS(A(K, L)))11, 12, 12
11 Z=ABS(A(K, L))
KP=K
12 CONTINUE

```

```

IF (L-KP) 13, 20, 20
13 DO 14 J=L,N
Z=A(L,J)
A(L,J)=A(KP,J)
14 A(KP,J)=Z
DO 15 J=1,N
Z=X(L,J)
X(L,J)=X(KP,J)
15 X(KP,J)=Z
20 IF (ABS(A(L,L))-EP) 50, 50, 30
30 IF (L-N) 31, 31, 34
31 LP1=L+1
DO 36 K=LP1,N
IF (A(K,L)) 32, 36, 32
32 RATIO=A(K,L)/A(L,L)
DO 33 J=LP1,N
33 A(K,J)=A(K,J)-RATIO*A(L,J)
DO 35 J=1,N
35 X(K,J)=X(K,J)-RATIO*X(L,J)
36 CONTINUE
34 CONTINUE
DO 43 I=1,N
II=N+1-I
DO 43 J=1,N
S=0.0
IF (II-N) 41, 43, 43
41 IIP1=II+1
DO 42 K=IIP1,N
42 S=S+A(II,K)*X(K,J)
43 X(II,J)=(X(II,J)-S)/A(II,II)
KER=1
DO 200 J=1,N
DO 200 K=1,N
200 CC(J,K)=X(J,K)
GO TO 75
50 KER=2
70 PRINT 71
71 FORMAT(1X, 'MATRIX SINGULAR IN GAUSD')
75 CONTINUE
RETURN
END
C ****SUBROUTINE THETA COMPUTES THE ANGLE OF ATTACK AND BANK
C ANGLES USING THE CHEBYSHEV POLYNOMIAL FORM FROM SJB.CHEBY.
SUBROUTINE THETA(T,UNM)
DIMENSION UNM(2)
COMMON/BP/BP(16)
COMMON/N/NE,NP,NPP1,NPP2
COMMON/TSH/TOT(8)

```

```

CALL CHEBY(T)
UNM(1)=0.0
DO 20 I=1,NPP1
20 UNM(1)=JNM(1)+BP(I+1)*TOT(I)
UNM(2)=0.0
DO 23 I=1,NPP2
23 UNM(2)=UNM(2)+BP(I+NPP1+1)*TOT(I)
RETURN
END
C ****SUBROUTINE CHEBY COMPUTES THE CHEBYSHEV POLYNOMIALS****
SUBROUTINE CHEBY(T)
COMMON/TSH/TOT(8)
TOT(1)=1.0
TOT(2)=2.0*T-1.0
TOT(3)=3.0*T**2-8.0*T+1.0
TOT(4)=32.0*T**3-48.0*T**2+18.0*T-1.0
TOT(5)=128.0*T**4-256.0*T**3+160.0*T**2-32.0*T+1.0
TOT(6)=512.0*T**5-1280.0*T**4+1120.0*T**3-400.0*T**2+50.0*T-1.0
TOT(7)=2048.0*T**6-8144.0*T**5+6312.0*T**4-3584.0*T**3
+640.0*T**2-72.0*T+1.0
TOT(8)=0.0
RETURN
END
C ****SUBROUTINE EOM COMPUTES THE INCLINATION CHANGE(DEG).
C IT USES THE CC6600 ROUTINE ODE TO DIFFERENTIATE THE
C EQUATIONS OF MOTION WHICH ARE CONTAINED IN SUBROUTINE F.
SUBROUTINE EOM(T,Y,DEG,INKCHG,IIP,SP)
EXTERNAL F
COMMON/B/B(10)
COMMON/BP/BP(16)
COMMON/N/NE,NP,NPP1,NPP2
COMMON J,RHO,VISC,REN,VEAR,PHI,CJEFDRG,COEFLFT
COMMON CDV,CLV,ARAY,V1,RA,DT
COMMON NOM
DIMENSION INKCHG(50)
DIMENSION CDV(8,12),CLV(8,12),ARAY(22,5),ZB(8)
DIMENSION Y(6),YP(6),WORK(250),IWORK(5),UNM(2)
REAL INKCHG
IIP=1
TTP=0.0
DO 2 I=1,6
2 Y(I)=Y(I)*1.0E+03
DO 3 I=1,6
3 ZB(I)=Y(I)
RELERR=1.0E-06
T=0.
TOUT=J.
IFLAG=1

```

```

KOUNT=0
1 CONTINUE
TOUT=T+DT
CALL ODE(F,6,Y,T,TOUT,RELERR,RELERR,IFLAG,WORK,IWORK)
IF(VBAR.LT.0.005) GO TO 50
IF(NOM-1.0) 48,44,44
48 CONTINUE
40 A1=ZB(2)*ZB(6)-ZB(3)*ZB(5)
B1=Y(2)*Y(6)-Y(3)*Y(5)
C1=ZB(3)*ZB(4)-ZB(1)*ZB(6)
D1=Y(3)*Y(4)-Y(1)*Y(6)
E1=ZB(1)*ZB(5)-ZB(2)*ZB(4)
F1=Y(1)*Y(5)-Y(2)*Y(4)
G=A1*B1+C1*D1+E1*F1
H=(A1**2+C1**2+E1**2)**0.5
O=(B1**2+D1**2+F1**2)**0.5
CI=G/(H*O)
IF(ABS(CI).GT.1.) CI=1.
AI=ACOS(CI)
DEG=AI*180.0/3.14159
IF(SP.GT.0.0) GO TO 736
IF(TOUT.GE.TTP) GO TO 735
GO TO 736
735 CONTINUE
INKCHG(IIP)=DEG
TTP=TTP+.05
IIP=IIP+1
736 DO 4 K=1,6
4 Y(K)=Y(K)*1.0E-03
VEL=(Y(4)**2+Y(5)**2+Y(6)**2)**.5
IF(TOUT.GE.1.0) GO TO 49
IF(KOUNT.GT.0) GO TO 45
PRINT*, "THIS IS NOMINAL DATA"
GO TO 46
45 IF(KOUNT.LT.50) GO TO 44
46 CONTINUE
APER=U/1000.
IF(KOUNT.GE.50) KOUNT=1
44 KOUNT=KOUNT+1
IF(TOUT.LE.1.0) GO TO 1
IF(TOUT.GE.1.0) GO TO 48
49 PRINT*, "THE GEOCENTRIC ALT IS ",RA
RETURN
50 PRINT*, "VBAR LESS THAN 0.005 ",VBAR
RETURN
END
C *****SUBROUTINE F CONTAINS THE EQUATIONS OF MOTION WHICH
C ARE USED BY ODE.

```

```

SUBROUTINE F(T,Y,YP)
COMMON U,PHO,VISC,REN,VBAR,PHI,COEFDRG,COEFLFT
COMMON CDV,CLV,ARAY,V1,FA,DT
COMMON/BP/BP(15)
DIMENSION Y(6),YP(6),CDV(8,12),CLV(8,12),ARAY(22,5),UNM(2)
GM=3.9852216E+14
OM=7.2921159E-05
SA=98.0
SM=97500.0
RA=(Y(1)**2+Y(2)**2+Y(3)**2)**.5
VS=Y(4)**2+Y(5)**2+Y(6)**2
V1=VS**.5
CALL AT40S(TM,WMOL)
CALL VISCAR(TM,WMOL)
CALL THETA(T,UNM)
CALL BIVINT(ALPHA,UNM)
PHI=UNM(2)
SPHI=SIN(PHI)
CPHI=COS(PHI)
SLIFT=.5*COEFLFT*SA*RHO*VS
DRAG=.5*COEFDRG*SA*RHO*VS
SLM=SLIFT/SM
SDM=DRAG/SM
AV=Y(4)-OM*Y(2)
BV=Y(5)+OM*Y(1)
CV=Y(5)
AH=BV*Y(3)-CV*Y(2)
BH=-(AV*Y(3)-CV*Y(1))
CH=AV*Y(2)-BV*Y(1)
AL=CV*BH-BV*CH
BL=-(CV*AH-CH*AV)
CL=BV*AH-BH*AV
SV=(AV**2+BV**2+CV**2)**.5
SH=(AH**2+BH**2+CH**2)**.5
SL=(AL**2+BL**2+CL**2)**.5
R3=(Y(1)**2+Y(2)**2+Y(3)**2)**1.5
YP(1)=Y(4)*BP(1)
YP(2)=Y(5)*BP(1)
YP(3)=Y(6)*BP(1)
YS4=-(GM/R3*Y(1))+SLM*(-SPHI*AH/SH+CPHI*AL/SL)-SDM*AV/SV
YP(4)=YS4*BP(1)
YS5=-(GM/R3*Y(2))+SLM*(-SPHI*BH/SH+CPHI*BL/SL)-SDM*BV/SV
YP(5)=YS5*BP(1)
YS6=-(GM/R3*Y(3))+SLM*(-SPHI*CH/SH+CPHI*CL/SL)-SDM*CV/SV
YP(6)=YS6*BP(1)
RETURN
END

```

```

C   ****SUBROUTINE ATMOS COMPUTES THE MOLEC.WEIGHT (WMOL) AND
C   DENISTY OF THE ATMOSPHERE
SUBROUTINE ATMOS(TM,WMOL)
COMMON U,RHO,VISC,REN,VBAR,PHI,COEFD RG,COEFLFT
COMMON CDV,CLV,ARAY,V1,RA,DT
DIMENSION CDV(8,12),CLV(8,12),ARAY(22,5)
GM=3.9852216E+14
R=8.31432E+03
RHOZ=1.2250
TMZ=288.15
U=RA-6356766.0
DO 7 M=1,22
IF (U-ARAY(M,1))5,6,7
7  CONTINUE
M=23
5  M=M-1
6  IF (ARAY(M,4))8,9,8
8  TM=ARAY(M,2)+ARAY(M,4)*(U-ARAY(M,1))
Q=GM*ARAY(M,5)/(R*RA**3)
SIGMA=EXP((1.0+(Q/ARAY(M,4)))*(ALOG(ARAY(M,2)/TM)))*ARAY(M,
-3)
GO TO 10
9  TM=ARAY(M,2)
Q=GM*ARAY(M,5)/(R*RA**2)
SIGMA=ARAY(M,3)*EXP(-(Q*(U-ARAY(M,1)))/ARAY(M,2))
10 RHO=RHOZ*SIGMA
WMOL=ARAY(M,5)
RETURN
END
C   ****SUBROUTINE VISC PAR COMPUTES VBAR****
SUBROUTINE VISC PAR(TM,WMOL)
COMMON U,RHO,VISC,REN,VBAR,PHI,COEFD RG,COEFLFT
COMMON CDV,CLV,ARAY,V1,RA,DT
DIMENSION CDV(8,12),CLV(8,12),ARAY(22,5)
T=TM*WMOL/28.9644
VISC=(1.458E-06*T**1.5)/(T+110.4)
REN=RHO*V1*32.77/VISC
A=SQRT(1.15*8.31432E+03*TM/28.9644)
TP=.458*T+1366.3+0.014625*((V1/A)**2)
EXP1=-5.0/T
EXP2=-5.0/TP
ANUM=T+122.1*10**EXP1
ADEN=TP+122.1*10**EXP2
CP=((TP/T)**.5)*ANUM/ADEN
VBAR=(V1/A)*(CP/REN)**.5
RETURN
END

```

```

C      *****SUBROUTINE BIVINT IS THE BIVARIANT INTERPOLATION SCHEME
C      USED TO GENERATED THE ORBITER COEFFICIENTS OF LIFT AND DRAG.
SUBROUTINE BIVINT(ALPHA,UNM)
COMMON U,RHO,VISC,KEN,VBAR,PHI,COEFD RG,COEFLFT
COMMON CDV,CLV,ARAY,V1,PA,DT
DIMENSION CDV(8,12),CLV(8,12),ARAY(22,5),UNM(2)
IF(VBAR.GT.5.2) GO TO 10
IF(UNM(1).LT.20.0) UNM(1)=20.0
IF(UNM(1).GT.50.0) UNM(1)=50.0
ALPHA=UNM(1)
DO 3 I=2,8
IF(ALPHA-CDV(I,1))2,2,3
3 CONTINUE
2 DA=CDV(I,1)-ALPHA
DO 5 J=2,12
IF(VBAR-CDV(1,J))4,4,5
5 CONTINUE
4 DV=CDV(1,J)-VBAR
DELV=CDV(1,J)-CDV(1,J-1)
P=DV/DELV
Q=DA/5.0
COEFD RG=(1-P)*(1-Q)*CDV(I,J)+P*(1-Q)*CDV(I,J-1)+Q*(1-P)*
-CDV(I-1,J)+P*Q*CDV(I-1,J-1)
DO 7 I=2,8
IF(ALPHA-CLV(I,1))6,6,7
7 CONTINUE
6 DA=CLV(I,1)-ALPHA
DO 9 J=2,12
IF(VBAR-CLV(1,J))8,8,9
9 CONTINUE
8 DV=CLV(1,J)-VBAR
DELV=CLV(1,J)-CLV(1,J-1)
P=DV/DELV
Q=DA/5.0
COEFLFT=(1-P)*(1-Q)*CLV(I,J)+P*(1-Q)*CLV(I,J-1)+Q*(1-P)*CLV
-(I-1,J)+P*Q*CLV(I-1,J-1)
GO TO 11
10 COEFD RG=0.0
COEFLFT=0.0
11 RETURN
END

```

-3238.565103448,5680.05361456,0.0
 -6.730633283745,-4.081365120586,0.0
 0.0,20.0,25.0,30.0,35.0,40.0,45.0,50.0
 .005,.18200,.27500,.43900,.61600,.82600,1.05800,1.3100
 .01,.1908,.2995,.4467,.6247,.8341,1.0669,1.3277
 .02,.20757,.31686,.45829,.63159,.84292,1.07501,1.33414
 .04,.232,.34142,.48176,.65264,.86123,1.09035,1.34628
 .06,.25643,.35607,.50532,.67309,.87946,1.1057,1.35837
 .08,.28087,.39053,.52879,.69474,.89777,1.12105,1.37052
 .31,.47782,.60696,.75822,.93047,1.13023,1.34592,1.58065
 .92,.88283,1.05234,1.23015,1.41531,1.60847,1.81111,2.01272
 1.65,1.15724,1.34469,1.54579,1.70485,1.89112,2.08391,2.26724
 2.5,1.27317,1.48087,1.68272,1.87878,2.06283,2.24867,2.4153
 5.05,1.37213,1.58875,1.80029,2.00107,2.18522,2.37206,2.53481
 5.2,1.39307,1.50633,1.82754,2.02903,2.22394,2.406,2.57175
 0.0,20.0,25.0,30.0,35.0,40.0,45.0,50.0
 .005,.34300,.50000,.64600,.78000,.89000,.97000,1.0290
 .01,.33757,.43527,.63669,.77082,.88415,.95735,1.02165
 .02,.33054,.48382,.62799,.75851,.8776,.96075,1.01556
 .04,.32155,.47237,.61444,.74377,.86224,.9454,1.00108
 .06,.31276,.45087,.60084,.72903,.84694,.93005,.98668
 .08,.30386,.44942,.58729,.71429,.83158,.91471,.9722
 .31,.26198,.38357,.49708,.60026,.69392,.75233,.80781
 .92,.17597,.24998,.31168,.36552,.41081,.44894,.46962
 1.65,.1095,.15051,.17679,.21991,.23799,.25831,.26259
 2.5,.07891,.10654,.11736,.12327,.12028,.12792,.12379
 5.05,.07203,.08448,.08759,.08208,.06883,.07029,.06102
 5.2,.08731,.10442,.10939,.10144,.09683,.08994,.08016

00000.,	288.65,	1.0000E+00,	-6.57E-08,	28.9644
11000.,	216.65,	2.9708E-01,	+0.00,	28.9644
20000.,	216.65,	7.1865E-02,	+1.0E-03,	28.9644
32000.,	228.65,	1.1055E-02,	+2.8E-03,	28.9644
47000.,	270.65,	1.1653E-03,	+0.0,	28.9644
52000.,	270.65,	6.1994E-04,	-2.0E-03,	28.9644
61000.,	252.65,	2.0497E-04,	-4.0E-03,	28.9644
79000.,	180.65,	1.9170E-05,	+0.0,	28.9644
90000.,	180.65,	2.5880E-06,	+3.0E-03,	28.9644
100000.,	210.65,	4.0600E-07,	+5.0E-03,	28.88
110000.,	260.65,	8.0280E-08,	+10.0E-03,	28.5E
120000.,	360.65,	1.9980E-08,	+20.0E-03,	28.07
150000.,	960.65,	1.498E-09,	+15.0E-03,	25.92
160000.,	1110.65,	9.459E-10,	+10.0E-03,	26.56
170000.,	1210.65,	6.560E-10,	+7.0E-03,	25.40
190000.,	1350.65,	3.548E-10,	5.0E-03,	25.85
230000.,	1550.65,	1.277E-10,	4.0E-03,	24.7
300000.,	1830.65,	2.926E-11,	3.3E-03,	22.66
400000.,	2160.65,	5.305E-12,	2.6E-03,	19.94
500000.,	2420.65,	1.287E-12,	+1.7E-03,	17.94
600000.,	2590.65,	3.787E-13,	1.1E-03,	16.34
700000.,	2700.65,	1.255E-13,	0.0,	15.17

VITA

Glenn S. Geary was born 11 May 1950 in Fairfield, California. He graduated from high school in Jerome, Arizona in 1968 and entered the United States Military Academy from which he received a Bachelor of Science degree in June 1972. Initially commissioned in the U.S. Army, he received an inter-service transfer to the U.S. Air Force in November 1975 and served as an Air Weapons Controller at Fort Monroe, Virginia and Osan AB, Korea before entering the School of Engineering, Air Force Institute of Technology, in June 1978.

Permanent Address: P.O. Box 360
Sedona, Arizona 86336

UNCLASSIFIED

SECURITY CLASSIFICATION OF THIS PAGE (When Data Entered)

REPORT DOCUMENTATION PAGE		READ INSTRUCTIONS BEFORE COMPLETING FORM
1. REPORT NUMBER AFIT/GA/AA/79D-4	2. GOVT ACCESSION NO.	3. RECIPIENT'S CATALOG NUMBER
4. TITLE (and Subtitle) USE OF AN AERODYNAMIC TURN TO MAXIMIZE THE ORBIT INCLINATION CHANGE FOR THE SPACE SHUTTLE ORBITER	5. TYPE OF REPORT & PERIOD COVERED MS THESIS	
	6. PERFORMING ORG. REPORT NUMBER	
7. AUTHOR(s)	8. CONTRACT OR GRANT NUMBER(s)	
9. PERFORMING ORGANIZATION NAME AND ADDRESS Air Force Institute of Technology (AFIT-EN) Wright-Patterson AFB, Ohio 45433		10. PROGRAM ELEMENT, PROJECT, TASK AREA & WORK UNIT NUMBERS
11. CONTROLLING OFFICE NAME AND ADDRESS	12. REPORT DATE December, 1979	
	13. NUMBER OF PAGES 81	
14. MONITORING AGENCY NAME & ADDRESS (if different from Controlling Office)	15. SECURITY CLASS. (of this report) Unclassified	
	15a. DECLASSIFICATION/DOWNGRADING SCHEDULE	
16. DISTRIBUTION STATEMENT (of this Report) Approved for public release; distribution unlimited		
17. DISTRIBUTION STATEMENT (of the abstract entered in Block 20, if different from Report) JOSEPH R. HIPPS, Major, USAF Director of Public Affairs		
18. SUPPLEMENTARY NOTES		
19. KEY WORDS (Continue on reverse side if necessary and identify by block number) Space Shuttle Orbiter Skip Reentry Orbiter Aerodynamics Optimal Control		
20. ABSTRACT (Continue on reverse side if necessary and identify by block number) Previous studies have shown that the Space Shuttle Orbiter can achieve larger orbit inclination changes using an aerodynamic turn than can be obtained using a rocket motor burn. This analysis determines the angle of attack and bank angle histories which maximize the change in inclination angle while satisfying final altitude and velocity loss constraints. The angle of attack and bank angle are modelled as polynomial functions of time with		

DD FORM 1473
1 JAN 73

EDITION OF 1 NOV 65 IS OBSOLETE

UNCLASSIFIED

SECURITY CLASSIFICATION OF THIS PAGE (When Data Entered)

UNCLASSIFIED

SECURITY CLASSIFICATION OF THIS PAGE(When Data Entered)

↓
unknown coefficients. The optimumⁿ values of the coefficients are determined by a gradient optimization technique.. Additionally, the sensitivity of the change in inclination angle to changes in the orbit apogee altitude is examined. It is shown that the Space Shuttle Orbiter can obtain higher inclination angle changes with higher apogee altitudes.
↑

UNCLASSIFIED

SECURITY CLASSIFICATION OF THIS PAGE(When Data Entered)